OPEN ACCESS

Original research

QRS complex and T wave planarity for the efficacy prediction of automatic implantable defibrillators

Katerina Hnatkova,[1] Irena Andršová ,[2,3] Tomáš Novotný,[2,3] Bert Vanderberk,[4] David Sprenkeler,[5] Juhani Junttila,[6] Tobias Reichlin,[7] Simon Schlögl,[8,9] Marc A Vos,[5] Tim Friede,[9,10] Axel Bauer,[11] Heikki V Huikuri,[12] Rik Willems,[13,14] Georg Schmidt,[15] Christian Sticherling,[16] Markus Zabel,[9,17] Marek Malik [1,2,3]

► Additional supplemental material is published online only. To view, please visit the journal online (http://dx.doi.org/10.1136/heartjnl-2023-322878).

For numbered affiliations see end of article.

Correspondence to
Professor Marek Malik, National Heart and Lung Institute, Imperial College London, London, W12 0NN, UK; marek.malik@imperial.ac.uk

Received 16 May 2023
Accepted 19 August 2023
Published Online First 15 September 2023

ABSTRACT

Objective To test the hypothesis that in recipients of primary prophylactic implantable cardioverter-defibrillators (ICDs), the non-planarity of ECG vector loops predicts (a) deaths despite ICD protection and (b) appropriate ICD shocks.

Methods Digital pre-implant ECGs were collected in 1948 ICD recipients: 21.4% females, median age 65 years, 61.5% ischaemic heart disease (IHD). QRS and T wave three-dimensional loops were constructed using singular value decomposition that allowed to measure the vector loop planarity. The non-planarity, that is, the twist of the three-dimensional loops out of a single plane, was related to all-cause mortality (n=294; 15.3% females; 68.7% IHD) and appropriate ICD shocks (n=162; 10.5% females; 87.7% IHD) during 5-year follow-up after device implantation. Using multivariable Cox regression, the predictive power of QRS and T wave non-planarity was compared with that of age, heart rate, left ventricular ejection fraction, QRS duration, spatial QRS-T angle, QTc interval and T-peak to T-end interval.

Results QRS non-planarity was significantly ($p<0.001$) associated with follow-up deaths despite ICD protection with HR of 1.339 (95% CI 1.165 to 1.540) but was only univariably associated with appropriate ICD shocks. Non-planarity of the T wave loop was the only ECG-derived index significantly ($p<0.001$) associated with appropriate ICD shocks with multivariable Cox regression HR of 1.364 (1.180 to 1.576) but was not associated with follow-up mortality.

Conclusions The analysed data suggest that QRS and T wave non-planarity might offer distinction between patients who are at greater risk of death despite ICD protection and those who are likely to use the defibrillator protection.

WHAT IS ALREADY KNOWN ON THIS TOPIC

⇒ In normal physiological recordings, the vectorcardiographic loops of the QRS complex and of the T wave are known to be practically planar, that is, with no or only little three-dimensional twist. The non-planarity of the vectorcardiographic loops has previously been observed mainly in patients with ischaemic heart disease. Nevertheless, the extent of the twist of these loops has not been investigated in recipients of implantable cardioverter-defibrillators (ICDs) implanted for primary prophylactic reasons.

WHAT THIS STUDY ADDS

⇒ The spatial twist of the vectorcardiographic loops of the QRS complex and of the T wave is measurable not only based on standard 12-lead ECGs but also based on restricted electrode sets suitable for prolonged monitoring.

⇒ In primary prophylactic ICD recipients, the extent of the twist of the QRS complex and of the T wave was found to be an independent predictor of risk.

⇒ The twist of the QRS complex was found to predict both all-cause mortality and, to a lesser extent, appropriate ICD shocks.

⇒ The twist of the T wave strongly predicted appropriate ICD shocks.

HOW THIS STUDY MIGHT AFFECT RESEARCH, PRACTICE OR POLICY

⇒ The results of the study need to be replicated in independent datasets. If the results are confirmed in prospectively collected ECGs of primary prophylactic ICD recipients, the predictive value of the QRS and T wave spatial twists needs to be assessed in terms of the distinction between patients who do and do not benefit from ICD primary prophylaxis. Such investigations might eventually lead to a change in the selection of patients for ICD primary prophylaxis.

INTRODUCTION

QRS micro-fragmentation was recently proposed to characterise depolarisation abnormalities beyond the visual detection on standard 12-lead ECGs.[1] This characteristic was shown to provide an independent mortality predictor in different populations.[2] It was proposed that the QRS micro-fragmentation expresses localised irregularities of ventricular excitation and that these aberrations signify heart failure including the early subclinical stages.

The essential concept of micro-fragmentation assessment is based on the analysis of simultaneously recorded ECG leads (ie, of the eight mutually

Linked

► http://dx.doi.org/10.1136/heartjnl-2023-323232

Check for updates

To cite: Hnatkova K, Andršová I, Novotný T, *et al*. *Heart* 2024;**110**:178–187.

independent signals of the standard ECG recording). The use of standard clinical ECGs makes the QRS micro-fragmentation analysis widely applicable to different clinical settings. Nevertheless, reliance on multiple ECG leads makes it inapplicable to situations when fewer ECG leads are available, for example, monitoring systems, standard clinical Holters and wearable ECG devices.

It has previously been reported that in physiological ECG recordings, the vectorcardiographic (VCG) loops of the QRS complex are essentially planarly,[3] that is, that the three-dimensional QRS dipole moves practically in a single plane the orientation of which depends on the position of the organ. Similar observations were also made for the VCG loop of the T wave.[4]

Our understanding of the predictive power of QRS micro-fragmentation suggests that aberrations of the depolarisation sequence might also influence the three-dimensional QRS loop and twist it outside a single two-dimensional plane. Since the VCG loops might be, in principle, constructed from as few as three independent ECG leads, the non-planarity characteristics might be derived from limited electrode sets.

Being guided by these considerations, we tested the hypotheses that QRS complex and T wave non-planarity indices are factors predicting death despite defibrillator protection and appropriate shock therapy by implantable cardioverter-defibrillators (ICDs). These hypotheses were tested in the previously reported population of recipients of prophylactic ICDs collected within the retrospective part of the EU-CERT-ICD Study.[5]

METHODS

Population and follow-up data

As already published,[2 5] the EU-CERT-ICD Study included a retrospective part that collected data of ICD recipients implanted in different European centres for primary prophylactic reasons between 2000 and 2014. Baseline characteristics, including age at ICD implantation, pre-implantation left ventricular ejection fraction (LVEF), and the distinction between ischaemic and non-ischaemic heart disease, were collected at each centre. Follow-up data were also provided by participating centres and were quality controlled by the team of University Hospital of Basel, Switzerland.

In each case, the ICD programming corresponded to the clinical needs and to the standard practice of each centre. The follow-up data provided by individual centres included all-cause mortality and ICD shocks that were adjudicated to differentiate between appropriate and inappropriate shocks. For the purposes of this investigation, all-cause mortality and appropriate ICD shocks were used as two separate follow-up event categories. Time of survival was defined as the interval between the ICD implantation and death; patients who did not die were censored at the end of the follow-up by the relevant centre. For patients who experienced an appropriate ICD shock, the interval between the device implantation and the first such shock was considered. As with all-cause mortality, patients who did not experience an appropriate ICD shock were censored (for the purposes of ICD shock prediction) at the time of their death or at the follow-up end. For the purposes of this investigation, follow-up was restricted to the first 5 years after ICD implantation.

ECG recordings

Electronic 12-lead short-term ECGs were obtained in 1948 patients prior to ICD implantation (median 1 day before implantation, IQR 1–6 days). These patients constituted the population of this study and were collected and followed up at the Department of Cardiology, University Hospital of Basel, Switzerland (n=488); Department of Cardiology and Pneumology, University Medical Center, Göttingen, Germany (n=441); Department of Cardiovascular Sciences, University of Leuven, Belgium (n=361); University Central Hospital of Oulu, Finland (n=32); and Department of Medical Physiology, University Medical Center Utrecht, the Netherlands (n=626). The ECG recordings obtained at Oulu were of 8-second duration, other ECGs were of 10-second duration.

ECG measurement

As previously reported,[2] the signals of all the ECGs were converted to the same digital format, cubic spline resampled (where appropriate) to 1 kHz frequency and filtered. Automatic QRS detection was visually confirmed and used to construct representative median beatforms of each ECG lead. For each ECG, these representative beatforms of different leads were superimposed on the same isoelectric axis and previously described algorithms were used to detect QRS onset, QRS offset and T wave offset. In each ECG, the delineation positions were visually checked and, where appropriate, manually corrected using a computer display with a single millisecond precision.

Using these representative beatform delineations, QRS complex and QT interval durations were obtained. Heart rate was derived from the average of all RR intervals in the entire ECG. Using this heart rate, rate-corrected QTc intervals were derived by Fridericia formula. The T-peak to T-end (TpTe) intervals were measured in the vector magnitude of all 12 leads using a previously reported method.[6] Using also previously published technique,[4] spatial QRS-T angles were measured and expressed in degrees (between 0° and 180°).

Assessment of QRS and T wave planarity

The main plane of ECG vector movement was defined by the means of singular value decomposition (SVD) of the ECG signals. In the same way as previously used for the QRS micro-fragmentation expression, the SVD decomposing signals were obtained.[1] The first two components (see the online supplemental material for details) defined the main plane and the two-dimensional vector loop movement within this plane. The third component (orthogonal to the first two) expressed the contribution of the signal components that twisted the vector loop outside the main plane (figure 1). The relative extent (percentage) of the third component expressed the non-planarity (the twist) of the three-dimensional vector loop (figure 1).

Using this principle, two pairs of assessments of the planarity ECG components were computed. First, all algebraically independent leads of the source ECG (that is, leads I, II and V1–V6) were used to apply the SVD algorithm to the QRS complex (the signal between the verified QRS onset and offset) and to the T wave (the signal between the QRS offset and T wave offset).

Second, to model the situation of ECGs with restricted leads, only signals between electrodes V1 and V6 were considered. Potential differences between four electrodes defined three leads, namely V2-V1, V5-V2 and V6-V5 approximating signal acquisition by a chest belt. These three derived leads were subsequently processed by SVD and the same approach as described expressed the QRS and T wave planarity values.

Statistics and data presentation

Continuous data are presented as medians (IQR). Non-parametric Kruskal-Wallis, Kolmogorov-Smirnov and χ^2 tests

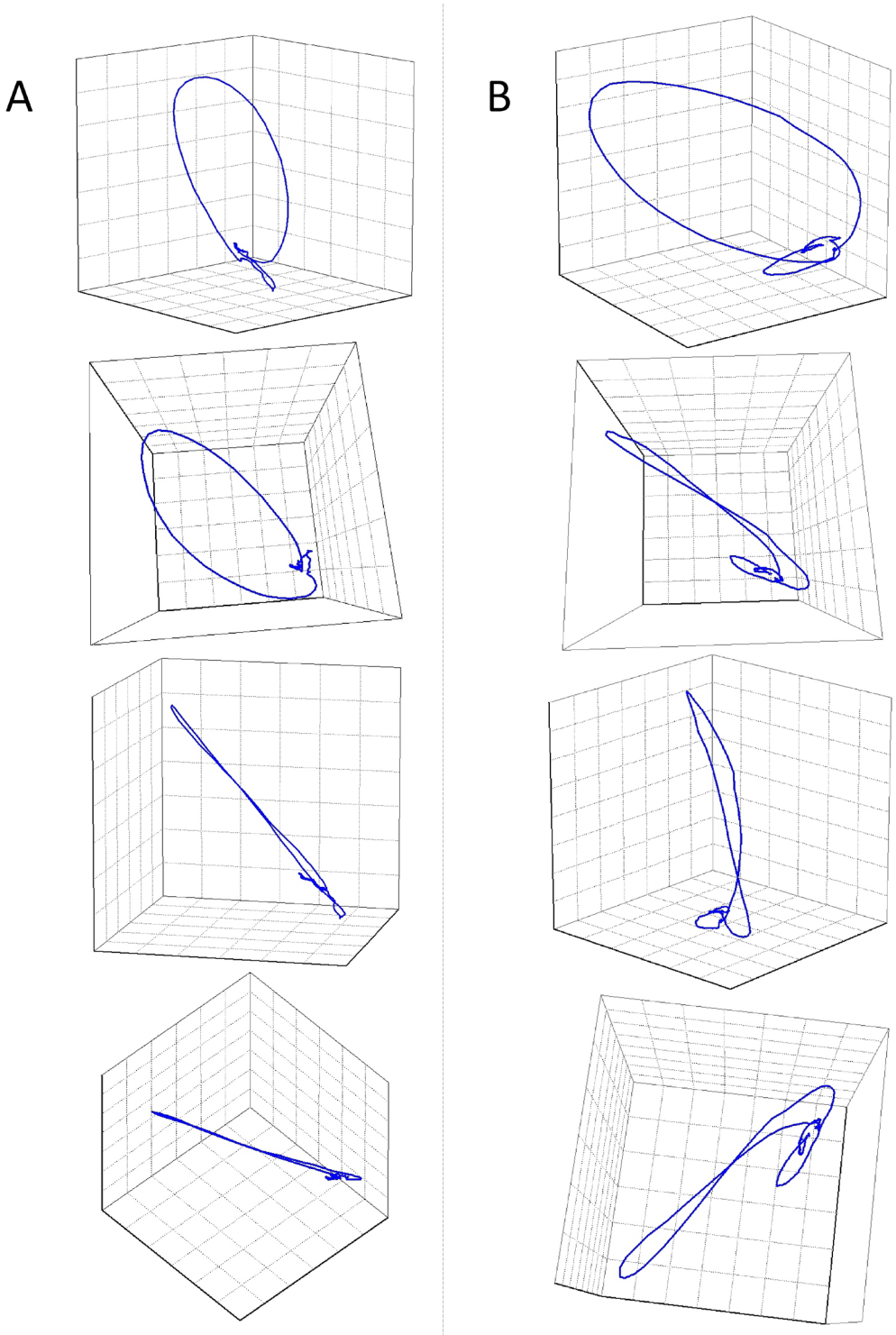

Figure 1 Examples of QRS planarity assessment. The images in each of the two columns of figure show different projections of three-dimensional QRS complex loops of ECGs of two different study subjects (ie, each column of the figure shows different views on the very same QRS complex loop), both around 70 years of age, with similar underlying heart rate and with the same QRS duration (see online supplemental material for the images of source ECGs). The images in (A) show that the loop of the QRS complex was planar, that is, that it collapses into a practically straight line when viewed from the side of the plane of the QRS vector movement. The QRS non-planarity (ie, the departures from the plane of the vector movement) was 2.17%; the patient survived the study follow-up. On the contrary, the images in (B) show that the loop of the QRS complex vector movement was twisted out of a single plane and that consequently, its three-dimensional nature was visible in all possible projections. The QRS non-planarity was 10.9% and the patient died 278 days after ICD implantation. The T wave planarity was assessed in the same way (note that small T wave loops are also visible in the images). Online supplemental material explains the techniques of the non-planarity measurements. Supplemental animations of the two QRS loops presented in the figure display the planarity and non-planarity differences of these two cases more clearly. The axes in the animations are the same as in the panels of this figure—in both ECGs; the axes were derived by singular value decomposition and subsequently rotated for display purposes. ICD, implantable cardioverter-defibrillator.

Table 1 Clinical characteristics

	No events in 5 years	Death in 5 years	ICD shock in 5 years	P value
N	1492	294	162	
Female sex	319 (21.4%)	45 (15.3%)	17 (10.5%)	0.002
Ischaemic HD	883 (59.2%)	202 (68.7%)	142 (87.7%)	0.003
Non-ischaemic HD	595 (39.9%)	86 (29.3%)	49 (30.2%)	0.007
CRT-D device implanted	589 (39.5%)	159 (54.1%)	73 (45.1%)	<0.001
Age (years)	64.0 (55.0–71.2)	69.3 (62.5–74.8)	63.8 (55.2–70.4)	<0.001
Heart rate (bpm)	69.0 (59.9–79.4)	72.9 (65.1–83.9)	68.0 (58.3–77.5)	<0.001
LVEF (%)	26 (21–31)	25 (20–30)	25 (20–31)	<0.001
QRS (ms)	127 (112–159)	146 (122–171)	131 (114–158)	<0.001
QRS-T angle (°)	151.3 (117.0–165.2)	159.9 (142.8–167.4)	148.3 (109.3–162.1)	<0.001
QRS n-pl (8 leads) (%)	4.49 (3.06–6.88)	5.59 (3.55–8.20)	5.21 (3.76–7.05)	<0.001
T wave n-pl (8 leads) (%)	2.87 (1.90–4.51)	3.06 (2.00–4.66)	3.55 (2.36–5.67)	<0.001
QRS n-pl (3 leads) (%)	4.34 (2.83–6.77)	6.00 (3.65–9.08)	4.55 (2.90–6.87)	<0.001
T wave n-pl (3 leads) (%)	3.03 (1.85–4.94)	3.32 (1.95–5.76)	3.85 (2.29–6.08)	0.001
QTc interval (ms)	442.2 (418.6–467.2)	452.4 (428.3–484.8)	442.1 (421.7–467.1)	<0.001
TpTe interval (ms)	97 (85–113)	98 (84–115)	96.5 (86–109)	0.928

The characteristics are shown for population subgroups stratified according to the events during 5-year follow-up (patients who experienced ICD shocks and subsequently died are included among those who died). Note that in 21 patients, the distinction between ischaemic and non-ischaemic HD was unclassified. The values shown are total count (percentage) for categorical variables, and median value (IQR) for continuous variables. The p values show χ^2 (for categorical variables) and Kruskal-Wallis (for continuous variables) comparisons of the distribution of the three study subgroups.
bpm, beats per minute; CRT-D, cardiac resynchronisation therapy-defibrillator; HD, heart disease; ICD, implantable cardioverter-defibrillator; LVEF, left ventricular ejection fraction; n-pl, non-planarity of the three-dimensional loop; TpTe, T-peak to T-end.

were used for group comparisons of continuous and categorical data, respectively. Non-parametric Spearman correlation coefficients were used to assess and test pairwise associations between continuous variables. Association of variables with outcome variables was tested by Cox regression analysis which was used both with single variables and for multivariable modelling with backwards stepwise elimination. For the purposes of Cox modelling of continuous variables, the QRS complex and T wave non-planarity values were logarithmically transformed. In addition to Cox regression analysis using continuous variables, models with

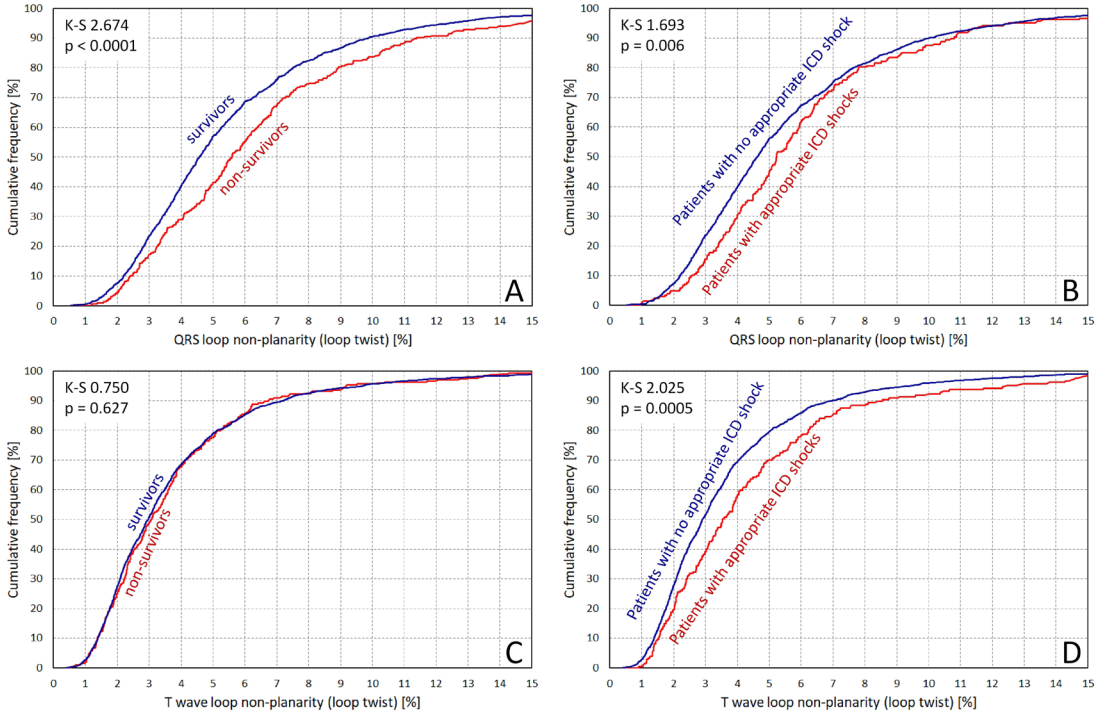

Figure 2 Comparison of QRS complex non-planarity values (A,B) and T wave non-planarity values (C,D) in patients who did and did not survive during the study follow-up (A and C) and in patients who experienced and did not experience appropriate ICD shocks (B and D). In each panel, cumulative distributions of the non-planarity values are shown together with Kolmogorov-Smirnov statistics and their corresponding p values. The non-planarity values shown were derived from the analysis of all eight independent leads of standard 12-lead ECGs. See the online supplemental material for the same comparison of non-planarity values derived from the ECG leads of the modelled chest belt (see the text for details). ICD, implantable cardioverter-defibrillator.

dichotomised variables were used. For this purpose, age was dichotomised at 75 years, heart rate at 75 beats/min, LVEF at 25% (close to the population median), QRS duration at 120 ms[7], QTc interval at 450 ms[8], TpTe interval at 100 ms[9] and QRS-T angle at 110°.[10] The QRS and T wave non-planarity values were dichotomised at their population medians. Two different datasets were used for multivariable Cox regression analysis. Model 1 tested available variables against the QRS complex and T wave non-planarity values derived from all original eight independent ECG leads; model 2 used QRS complex and planarity values derived from the modelled chest belt of electrodes V1, V2, V5 and V6. The association of the dichotomised non-planarity values with outcome was also tested by Kaplan-Meier survival curves; the differences between the curves were tested by log rank test.

SVD computation and the assessment of non-planarity of QRS complex and of T wave were programmed in C++ (Microsoft Visual Studio Professional 2022, 64-bit V.17.3.5). Statistical evaluation was performed by SPSS package (V.27; IBM Corporation); p values below 0.05 were considered statistically significant.

Additional analyses are described in the online supplemental material.

RESULTS

Of the 1948 patients of the study, 294 (15.1%) died during the follow-up restricted to the first 5 years. Defibrillators with cardiac resynchronisation therapy (CRT) function were implanted in 797 patients. In 57 patients (2.9%), the information on ICD shock therapy was not available. Among the remaining 1897 patients, 207 (10.9%) experienced an appropriate ICD shock during the first 5 years of follow-up. Of these, 45 patients (21.7% of patients who received a shock) subsequently died during the first 5 years of follow-up. Clinical characteristics of the population and the measured non-planarity values of ECG components are shown in table 1. Differences between non-planarity values in patients with and without follow-up events are shown in figure 2.

QRS non-planarity values assessed from original 12-lead ECGs and from the modelled chest belt electrodes were significantly correlated (Spearman's r=0.455, p<0.001). The same was true for the T wave non-planarity (r=0.429, p<0.001). QRS non-planarity values were also correlated with the QRS duration (r=0.204 and 0.189, both p<0.01, for the values derived from the original ECGs and from the chest belt electrodes, respectively). No significant correlations were found between the T wave non-planarity values and the QT interval duration (r=0.012 and r=−0.004, for the two sets of values, respectively). The correlations between the QRS non-planarity and T wave non-planarity were very modest (r=0.154 and r=0.202, respectively).

Table 2 shows the results of the Cox regression analysis based on the continuous variables. The departure from planarity of the QRS complex loop was found to be a strong predictor of all-cause mortality independent of other factors used in the model. While QRS duration and QTc duration were significantly associated

Table 2 Event prediction based on continuous variables

	Univariable analysis			Multivariable analysis: model 1 (8 leads)			Multivariable analysis: model 2 (3 leads)		
	Wald	P value	HR (95% CI)	Wald	P value	HR (95% CI)	Wald	P value	HR (95% CI)
Prediction of 5-year all-cause mortality									
Age (years)	**48.9**	**<0.001**	**1.043 (1.031 to 1.055)**	37.5	<0.001	1.038 (1.026 to 1.051)	32.0	<0.001	1.035 (1.023 to 1.048)
Heart rate (bpm)	**30.8**	**<0.001**	**1.019 (1.012 to 1.026)**	24.2	<0.001	1.018 (1.011 to 1.025)	19.5	<0.001	1.016 (1.009 to 1.024)
LVEF (%)	**30.1**	**<0.001**	**0.959 (0.945 to 0.973)**	11.4	0.001	0.972 (0.955 to 0.988)	11.7	0.001	0.972 (0.956 to 0.988)
QRS duration (ms)	**26.6**	**<0.001**	**1.009 (1.006 to 1.013)**						
QTc interval (ms)	**20.3**	**<0.001**	**1.006 (1.004 to 1.009)**						
QRS-T angle (°)	**26.1**	**<0.001**	**1.010 (1.006 to 1.014)**	8.88	0.003	1.006 (1.002 to 1.010)	8.13	0.004	1.006 (1.002 to 1.010)
TpTe interval (ms)	1.09	0.296	1.002 (0.998 to 1.006)						
$\log_2$ (QRS n-pl 8 leads)	**17.5**	**<0.001**	**1.329 (1.163 to 1.519)**	16.8	<0.001	1.339 (1.165 to 1.540)			
$\log_2$ (T wave n-pl 8 leads)	0.87	0.349	1.061 (0.938 to 1.200)						
$\log_2$ (QRS n-pl 3 leads)	**35.0**	**<0.001**	**1.437 (1.275 to 1.621)**				20.6	<0.001	1.338 (1.180 to 1.517)
$\log_2$ (T wave n-pl 3 leads)	3.39	0.066	1.109 (0.993 to 1.237)						
Prediction of 5-year ICD shocks									
Age (years)	0.43	0.510	1.004 (0.992 to 1.016)						
Heart rate (bpm)	1.73	0.188	0.994 (0.984 to 1.003)						
LVEF (%)	0.01	0.975	1.000 (0.985 to 1.014)						
QRS duration (ms)	0.23	0.879	1.000 (0.995 to 1.004)						
QTc interval (ms)	0.15	0.696	1.001 (0.997 to 1.004)						
QRS-T angle (°)	0.91	0.340	0.998 (0.995 to 1.002)						
TpTe interval (ms)	0.50	0.476	0.998 (0.992 to 1.004)						
$\log_2$ (QRS n-pl 8 leads)	**6.61**	**0.010**	**1.233 (1.051 to 1.447)**						
$\log_2$ (T wave n-pl 8 leads)	**17.7**	**<0.001**	**1.364 (1.180 to 1.576)**	17.7	<0.001	1.364 (1.180 to 1.576)			
$\log_2$ (QRS n-pl 3 leads)	1.33	0.249	1.087 (0.943 to 1.253)						
$\log_2$ (T wave n-pl 3 leads)	**4.96**	**0.026**	**1.159 (1.018 to 1.321)**				4.96	0.026	1.159 (1.018 to 1.321)

Univariable and multivariable (backwards stepwise elimination) Cox regression analyses for the prediction of outcome events during 5-year follow-up (see the text for the distinction of the two multivariable models). Risk factors entered as continuous variables, n-pl indices of QRS and T wave loops entered after logarithmic transformation. Statistically significant results are shown in bold. In addition to the p values, the levels of Wald statistics are also shown. The grey areas indicate the variables excluded in the different multivariable models.
bpm, beats per minute; ICD, implantable cardioverter-defibrillator; LVEF, left ventricular ejection fraction; n-pl, non-planarity; TpTe, T-peak to T-end.

Table 3 Event prediction based on dichotomised and categorical variables

	Univariable analysis			Multivariable analysis: model 1 (8 leads)			Multivariable analysis: model 2 (3 leads)		
	Wald	P value	HR (95% CI)	Wald	P value	HR (95% CI)	Wald	P value	HR (95% CI)
Prediction of 5-year all-cause mortality									
Age >75 years	**32.6**	**<0.001**	**2.181 (1.669 to 2.850)**						
Female sex	0.51	0.476	0.891 (0.648 to 1.224)						
Non-ischaemic aetiology	2.32	0.127	0.834 (0.660 to 1.053)						
CRT-D device implanted	**21.0**	**<0.001**	**1.710 (1.360 to 2.152)**						
Heart rate >75 bpm	**19.7**	**<0.001**	**1.685 (1.338 to 2.121)**	8.00	0.005	2.956 (1.392 to 6.274)	8.06	0.005	2.973 (1.401 to 6.305)
LVEF <25%	**14.5**	**<0.001**	**1.563 (1.241 to 1.967)**						
QRS duration >120 ms	**24.9**	**<0.001**	**2.010 (1.528 to 2.643)**						
QTc >450 ms	**8.05**	**0.005**	**1.393 (1.108 to 1.752)**						
QRS-T angle >110°	**14.2**	**<0.001**	**1.554 (1.235 to 1.954)**						
TpTe >100 ms	0.17	0.895	0.985 (0.783 to 1.238)						
QRS n-pl 8 leads >median	**20.4**	**<0.001**	**1.730 (1.364 to 2.193)**	7.19	0.007	3.051 (1.350 to 6.894)			
T wave n-pl 8 leads >median	0.81	0.367	1.111 (0.884 to 1.397)						
QRS n-pl 3 leads >median	**33.2**	**<0.001**	**2.034 (1.598 to 2.589)**				7.78	0.005	3.189 (1.413 to 7.204)
T wave n-pl 3 leads >median	0.95	0.329	1.121 (0.891 to 1.410)						
Prediction of 5-year ICD shocks									
Age >75 years	0.20	0.655	0.909 (0.598 to 1.381)						
Female sex	**7.55**	**0.006**	**0.538 (0.346 to 0.837)**	7.48	0.006	0.539 (0.346 to 0.840)	7.08	0.008	0.548 (0.352 to 0.854)
Non-ischaemic aetiology	**3.97**	**0.046**	**0.751 (0.566 to 0.995)**						
CRT-D device implanted	3.29	0.070	0.768 (0.577 to 1.021)						
Heart rate >75 bpm	2.35	0.125	0.790 (0.584 to 1.068)						
LVEF <25%	<0.01	0.989	1.002 (0.755 to 1.330)						
QRS duration >120 ms	1.65	0.199	1.209 (0.905 to 1.614)						
QTc >450 ms	0.24	0.623	0.933 (0.708 to 1.230)						
QRS-T angle >110°	0.70	0.404	0.888 (0.672 to 1.173)						
TpTe >100 ms	**4.33**	**0.037**	**0.743 (0.562 to 0.983)**						
QRS n-pl 8 leads >median	**11.2**	**0.001**	**1.609 (1.217 to 2.128)**	8.93	0.003	1.536 (1.159 to 2.035)			
T wave n-pl 8 leads >median	**12.2**	**<0.001**	**1.647 (1.245 to 2.180)**	9.52	0.002	1.559 (1.176 to 2.067)			
QRS n-pl 3 leads >median	2.76	0.097	1.261 (0.959 to 1.658)						
T wave n-pl 3 leads >median	**5.43**	**0.020**	**1.389 (1.054 to 1.832)**				5.38	0.020	1.389 (1.052 to 1.833)

Univariable and multivariable (backwards stepwise elimination) Cox regression analyses for the prediction of outcome events during 5-year follow-up (see the text for the distinction of the two multivariable models). Risk factors entered as dichotomised variables, n-pl indices of QRS and T wave loops stratified according to population median. Statistically significant results are shown in bold. In addition to the p values, the levels of Wald statistics are also shown. The grey areas indicate the variables excluded in the different multivariable models.
bpm, beats per minute; CRT-D, cardiac resynchronisation therapy-defibrillator; ICD, implantable cardioverter-defibrillator; LVEF, left ventricular ejection fraction; n-pl, non-planarity; TpTe, T-peak to T-end.

with mortality univariably, they were not found significant in a multivariable analysis. Both the departures from QRS planarity assessed in the complete 12-lead ECG and in the precordial band predicted the mortality strongly.

Interestingly, the departure from the planarity of the T wave loop (regardless of whether assessed in the complete ECG or in the precordial band) was the only significant predictor of appropriate ICD shocks that was not eliminated in the multivariable models. QRS planarity assessed from the complete 12-lead ECG was also a univariable predictor of ICD shocks but, in a multivariable analysis, it was eliminated when the T wave loop non-planarity was included.

Consistent results were found with Cox regression models based on dichotomised variables (table 3). When including the distinction between CRT/non-CRT defibrillators, only increased heart rate and QRS non-planarity survived in the multivariable models of mortality prediction.

As expected, female sex was strongly associated with the absence of ICD shocks which remained in the multivariable models when the absence of planarity of the T wave (assessed in either way) was added to the model. Univariably but not multivariably, non-ischaemic heart disease predicted fewer ICD shocks. Interestingly, the TpTe interval above 100 ms was also found significantly associated with the ICD shocks but, contrary to expectations, it predicted fewer rather than more frequent shocks. It did not remain significant in multivariable models.

Figures 3 and 4 show the distinction of Kaplan-Meier curves of probability of follow-up events when dividing the population according to QRS complex and T wave loop planarity. All the distinctions were consistent with the univariable results in table 2.

Additional results are described in the online supplemental material.

DISCUSSION

The analyses show that the non-planarity of the three-dimensional QRS complex and T wave loops provides risk assessment independently of other risk factors.

Physiologically, these observations make sense. Depolarisation abnormalities have repeatedly been associated with poorer survival of cardiac patients[11–13] and QRS complex abnormalities

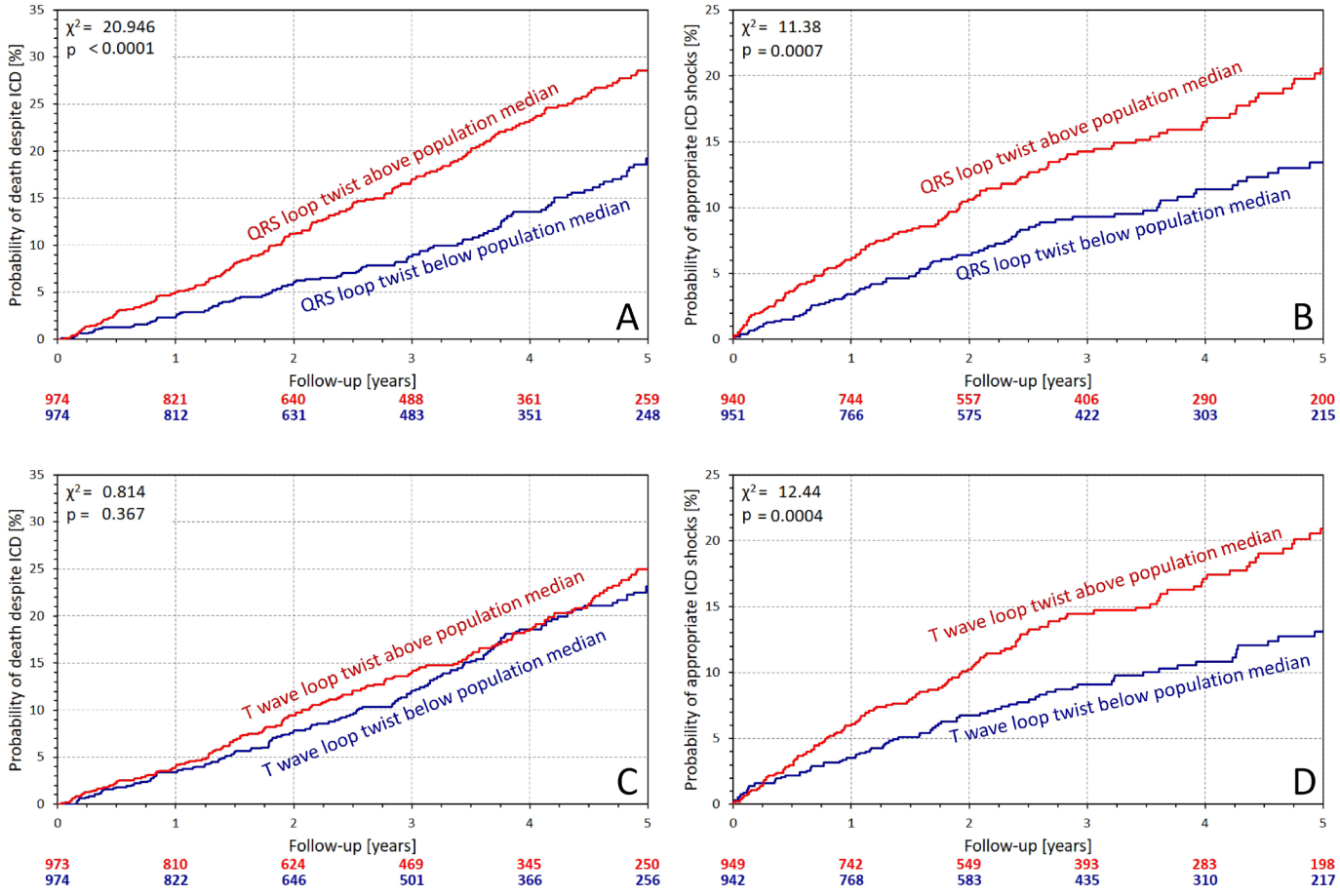

Figure 3 Kaplan-Meier analysis of the probability of death despite ICD protection (A and C) and of the probability of first appropriate ICD shock (B and D). (A,B) Comparison of the subgroups stratified by QRS complex non-planarity (QRS loop twist); (C,D) comparison of the subgroups stratified by the T wave non-planarity (T wave loop twist). The characteristics used in the comparisons were derived from eight independent leads of the complete ECG recordings. χ^2 statistics and corresponding p values comparing the Kaplan-Meier curves are shown in each panel. The number of patients at risk in these groups is shown below the panels in colours corresponding to the individual graphs. Note that the data on ICD shocks were not available for the complete population—see the text for details. ICD, implantable cardioverter-defibrillator.

have been reported to predict heart failure complications more strongly compared with the arrhythmia prediction. Conversely, repolarisation anomalies have repeatedly been associated with arrhythmic complications and sudden cardiac death.[14–16]

The measurement of QRS non-planarity is mathematically independent of the assessment of QRS micro-fragmentation.[1] We have indeed seen occasional ECGs in which minimal QRS non-planarity was combined with substantial micro-fragmentation and vice versa. Nevertheless, when both QRS non-planarity and QRS micro-fragmentation were used in Cox regression models predicting mortality, the non-planarity was eliminated in the multivariable analysis irrespective of whether continuous or dichotomised variables were used (details not shown). It thus seems that QRS non-planarity, while technically independent, provides less powerful detection of depolarisation abnormalities, although it might be assessed from a limited number of ECG leads. It remains to be seen whether in other populations, QRS non-planarity would significantly contribute to mortality risk predicted by QRS micro-fragmentation.

Since the T wave non-planarity was the only ECG-related parameter that significantly predicted ICD shocks, more advanced analyses of multilead T wave signals of standard ECGs are of interest. Nevertheless, when applying the algorithm of QRS micro-fragmentation to the T wave analysis, we have not obtained any significant prediction of mortality and/or of ICD shocks (details not shown). This is not surprising since propagation of myocardial repolarisation changes is influenced by intercellular electronic interactions[17] that eliminate abnormalities that would be detectable by the micro-fragmentation analyses. Nevertheless, different analyses of T wave signals might classify pro-arrhythmic abnormalities of the repolarisation sequence more powerfully compared with the simple non-planarity assessment.

Although the measurements of the QRS and T wave non-planarity in full 12-lead ECGs and in the modelled chest belt were significantly correlated, numerical differences were noticeable. This is not surprising. The SVD analysis represents the multilead ECG signal by a multidimensional vector movement which is a simplification of the electrophysiological processes in the complete organ. Irrespective of this simplification, analyses of both electrode configurations led to similar predictions of follow-up events.

The four electrodes that we selected to model a chest belt are not arranged along a true circle which is of advantage when studying three-dimensional ECG signal properties. The three leads that we obtained from these electrodes were selected arbitrarily since any other combinations (eg, V1–V2, V1–V5 and V1–V6) are only algebraic combinations of the used leads and would thus provide the same SVD decomposition results.

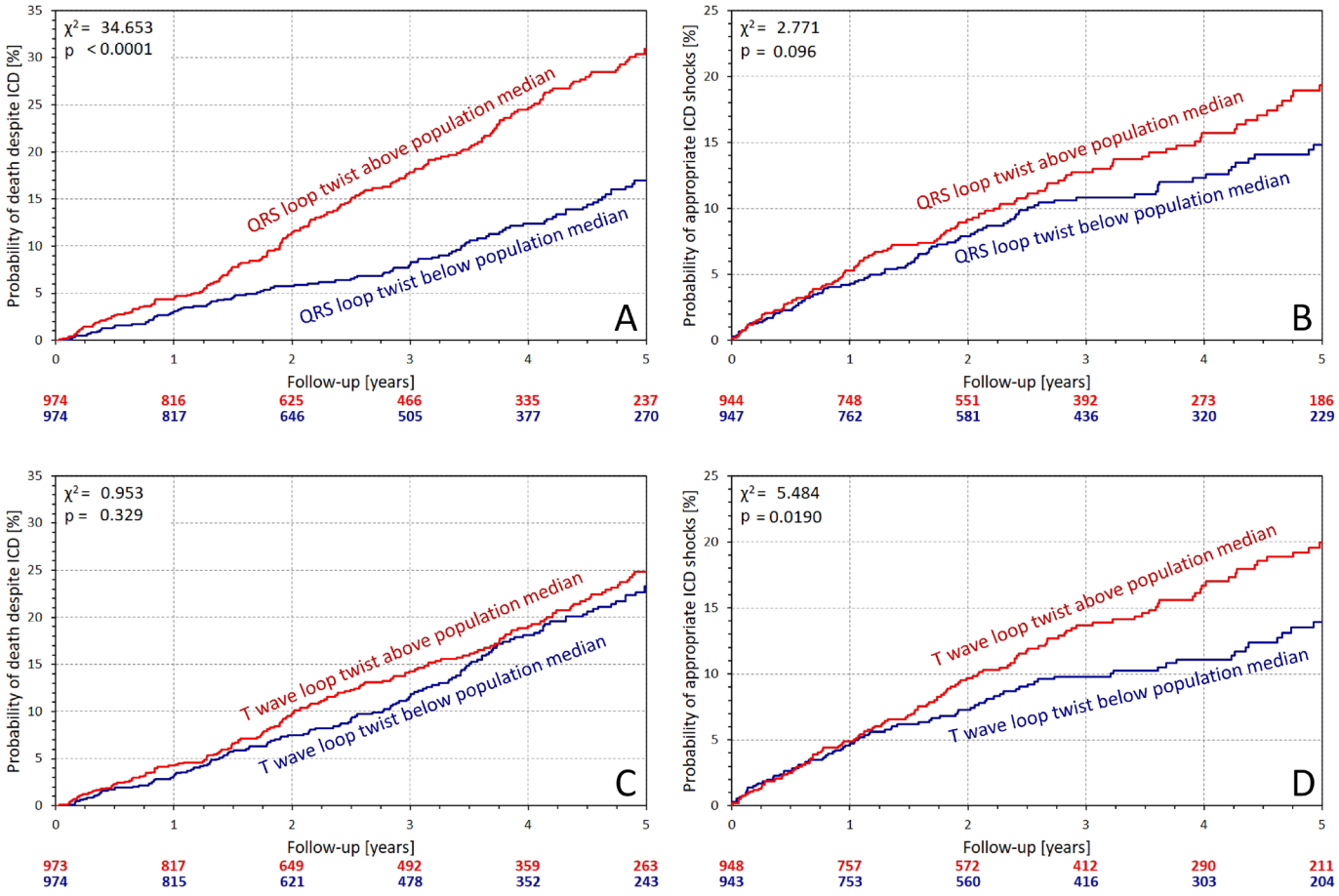

Figure 4 Kaplan-Meier analysis of the probability of death despite ICD protection (A and C) and of the probability of first appropriate ICD shock (B and D). (A,B) Comparison of the subgroups stratified by QRS complex non-planarity (QRS loop twist); (C,D) comparison of the subgroups stratified by the T wave non-planarity (T wave loop twist). The characteristics used in the comparisons were derived from three leads modelling a chest belt (see the text for details). χ^2 statistics and corresponding p values comparing the Kaplan-Meier curves are shown in each panel. The number of patients at risk in these groups is shown below the panels in colours corresponding to the individual graphs. Note that the data on ICD shocks were not available for the complete population—see the text for details. ICD, implantable cardioverter-defibrillator.

Multiple studies investigated the planarity and non-planarity of the QRS complex. The planarity was assessed mainly in VCG using different expressions including the length, width, thickness, and thickness/length and width/length ratios of the QRS loop in different spatial projections.[18] The QRS non-planarity has previously been investigated mainly in relation to ischaemic heart disease and myocardial infarction.[3 18 19] Although about 60% of the patients of the study suffered from ischaemic heart disease, multivariable Cox regression analysis showed that the predictive value of QRS loop non-planarity was independent of heart disease aetiology. T wave loop abnormalities have also been repeatedly studied using different characteristics.[4 20] Among others, T wave-based prediction of mortality in ischaemic heart disease was repeatedly reported.[21–23] Interestingly, in pilot data that preceded the EU-CERT-ICD Study, Seegers *et al*[24] reported that pre-implantation T wave area predicted appropriate ICD shocks. Of these studies, T wave loop planarity was sparsely investigated, mainly in ischaemic heart disease.[18]

Naturally, every retrospective analysis can only be hypothesis generating. Nevertheless, if our findings are independently confirmed in independent datasets, the assessment of QRS and T loop planarity might be of assistance when considering ICD implantation in patients at the border of criteria of the ICD guidelines. Patients in whom a flat QRS complex loop is combined with a twisted T wave loop might be stronger candidates for ICD prophylaxis compared with patients in whom the planarity of the QRS complex and T wave loops appears to be the other way round. Still, independent confirmations of this possibility are needed before any clinical utility might be proposed.

In future ECG studies, combination of the non-planarity indices of ECG loops needs to be investigated together with other ECG factors[25] including those that were derived from long-term recordings[26] which were not available for the retrospective EU-CERT-ICD dataset. Analyses of longer recordings, applicable to both monitoring systems and ECG wearables, would also allow to address the variability and intrasubject reproducibility[27] of the non-planarity indices.

LIMITATIONS

The available data were limited in several aspects; distinction between cardiac and non-cardiac, and sudden and non-sudden death was not available. While it might be assumed that among prophylactic ICD recipients, mortality was mainly cardiac/cardiovascular, the lack of distinction between sudden and thus presumably arrhythmic and non-sudden deaths prevented us from some more detailed investigations, for example, of the MADIT ICD benefit score.[28] It might only be assumed that in patients under ICD protection, most cardiac deaths are related to heart failure. CRT utilisation data are not available. Having

only one ECG recording in each patient did not allow us to study measurement reproducibility. In the Cox regression analysis, we have intentionally included mostly parameters that might be obtained from ECG analysis. Additional clinical findings, for example, electrophysiological investigation (not available in the investigated dataset), might outperform the risk prediction by the reported indices, although they would not have the advantage of undemanding data acquisition. Finally, these retrospective results have not been tested prospectively. We plan to perform such a prospective evaluation once the follow-up data of the prospective part of the EU-CERT-ICD Study[29] have been extended; this follow-up extension is presently ongoing.

CONCLUSIONS

Despite these limitations, the study shows that the assessment of QRS complex and T wave loop planarity might also be obtained from limited electrode sets. This makes the assessment plausible also based on data from monitoring systems and wearable devices. In patients with ICD implanted for prophylactic reasons, the estimates of QRS complex and T wave loop planarity appear to differ between those who do and do not use the cardioversion function as well those who do and do not survive despite the ICD anti-tachycardia protection.

Author affiliations
[1]National Heart and Lung Institute, Imperial College London, London, UK
[2]Department of Internal Medicine and Cardiology, University Hospital Brno, Brno, Czech Republic
[3]Department of Internal Medicine and Cardiology, Masaryk University, Brno, Czech Republic
[4]Department of Cardiovascular Sciences, University of Leuven, Leuven, Belgium
[5]Department of Medical Physiology, University Medical Center Utrecht, Utrecht, The Netherlands
[6]MRC Oulu, University Central Hospital of Oulu and University of Oulu, Oulu, Finland
[7]Department of Cardiology, Inselspital, Bern University Hospital, Bern, Switzerland
[8]Department of Cardiology and Pneumology, University Medical Center Göttingen, Gottingen, Germany
[9]German Center of Cardiovascular Research (DZHK), partner site Göttingen, Göttingen, Germany
[10]Department of Medical Statistics, University Medical Center Göttingen, Göttingen, Germany
[11]University Hospital for Internal Medicine III, Medical University Innsbruck, Innsbruck, Austria
[12]University Central Hospital of Oulu and University of Oulu, Oulu, Finland
[13]Division of Experimental Cardiology, Department of Cardiovascular Diseases, University of Leuven, Leuven, Belgium
[14]Division of Clinical Cardiology, University Hospitals Leuven, Leuven, Belgium
[15]Medizinische Klinik, Klinikum rechts der Isar der Technischen Universität München, Munich, Germany
[16]Department of Cardiology, University Hospital of Basel, Basel, Switzerland
[17]Cardiology and Pneumology, Heart Center, University Hospital Göttingen, Göttingen, Germany

Contributors KH—conceptual design of the study, ECG processing algorithms, software coding and computer implementation of ECG analyses, algorithmic measurements of relevant ECG intervals, application of the analytical methods to the EU-CERT-ICD WP02 database of ECG signals, interpretation of results, manuscript draft, manuscript revisions, approval of individual manuscript versions; member of the EU-CERT-ICD Study team. IA—conceptual design of the study, comments to the algorithmic measurements of ECG intervals, visual verification of the measurements of relevant ECG intervals, manual correction of the measurements of relevant ECG intervals, quality control of ECG measurements, interpretation of results, manuscript draft, approval of individual manuscript versions. TN—comments to the algorithmic measurements of ECG intervals, visual verification of the measurements of relevant ECG intervals, manual correction of the measurements of relevant ECG intervals, quality control of ECG measurements, interpretation of results, manuscript draft, approval of individual manuscript versions; member of the EU-CERT-ICD Study team. BV—collection of ECG signals contributed by the Leuven team to the ECG part of the WP02 database of EU-CERT-ICD, submission of these ECGs for study analyses, quality control of the Leuven part of the EU-CERT-ICD WP02 ECGs after their conversion into a common open format, follow-up of the Leuven patients submitted to the retrospective WP02 part of EU-CERT-ICD, comments to the manuscript, approval of the final manuscript; member of the EU-CERT-ICD Study team. DS—collection of ECG signals contributed by the Utrecht team to the ECG part of the WP02 database of EU-CERT-ICD, submission of these ECGs for study analyses, quality control of the Utrecht part of the EU-CERT-ICD WP02 ECGs after their conversion into a common open format, follow-up of the Utrecht patients submitted to the retrospective WP02 part of EU-CERT-ICD, comments to the manuscript, approval of the final manuscript; member of the EU-CERT-ICD Study team. JJ—collection of ECG signals contributed by the Oulu team to the ECG part of the WP02 database of EU-CERT-ICD, submission of these ECGs for study analyses, quality control of the Oulu part of the EU-CERT-ICD WP02 ECGs after their conversion into a common open format, comments to the algorithmic measurements of ECG intervals, follow-up of the Oulu patients submitted to the retrospective WP02 part of EU-CERT-ICD, quality control of the Oulu part of the EU-CERT-ICD WP02 database, comments to the manuscript, approval of the final manuscript; member of the EU-CERT-ICD Study team. TR—collection of ECG signals contributed by the Basel team to the ECG part of the WP02 database of EU-CERT-ICD, submission of these ECGs for study analyses, quality control of the Basel part of the EU-CERT-ICD WP02 ECGs after their conversion into a common open format, follow-up of the Basel patients submitted to the retrospective WP02 part of EU-CERT-ICD, comments to the manuscript, approval of the final manuscript. SS—collection of ECG signals contributed by the Göttingen team to the ECG part of the WP02 database of EU-CERT-ICD, submission of these ECGs for study analyses, quality control of the Göttingen part of the EU-CERT-ICD WP02 ECGs after their conversion into a common open format, follow-up of the Göttingen patients submitted to the retrospective part of EU-CERT-ICD, comments to the manuscript, approval of the final manuscript; member of the EU-CERT-ICD Study team. MAV—collection of ECG signals contributed by the Utrecht team to the ECG part of the WP02 database of EU-CERT-ICD, submission of these ECGs for study analyses, quality control of the Utrecht part of the EU-CERT-ICD WP02 ECGs after their conversion into a common open format, follow-up of the Utrecht patients submitted to the retrospective WP02 part of EU-CERT-ICD, quality control of the Utrecht part of the EU-CERT-ICD WP02 database, comments to the manuscript, approval of the final manuscript; member of the EU-CERT-ICD Study team. TF—statistical aspects of the study design concept, statistical consultations, models of the EU-CERT-ICD WP02 data collection, quality control of the complete EU-CERT-ICD WP02 database, quality control of the ECG links to the EU-CERT-ICD WP02 database, approval of the statistical methods of the data analyses used in the manuscript, comments to the manuscript, approval of the final manuscript; member of the EU-CERT-ICD Study team. AB—concepts of ECG data analyses, physiological interpretation of ECG analyses and of their measurement results, design and completeness control of the data analyses, interpretation of results, manuscript draft, manuscript revisions, approval of the final manuscript; member of the EU-CERT-ICD Study team. HVH—collection of ECG signals contributed by the Oulu team to the ECG part of the WP02 database of EU-CERT-ICD, submission of these ECGs for study analyses, quality control of the Oulu part of the EU-CERT-ICD WP02 ECGs after their conversion into a common open format, comments to the initial algorithmic measurements of ECG intervals, quality control of the initial algorithmic measurements of ECG intervals, follow-up of the Oulu patients submitted to the retrospective part of EU-CERT-ICD, quality control of the Oulu part of the EU-CERT-ICD WP02 database, comments to the manuscript, approval of the final manuscript; member of the EU-CERT-ICD Study team. RW—collection of ECG signals contributed by the Leuven team to the ECG part of the WP02 database of EU-CERT-ICD, submission of these ECGs for study analyses, quality control of the Leuven part of the EU-CERT-ICD WP02 ECGs after their conversion into a common open format, comments to the initial algorithmic measurements of ECG intervals, quality control of the initial algorithmic measurements of ECG intervals, follow-up of the Leuven patients submitted to the retrospective part of EU-CERT-ICD, quality control of the Leuven part of the EU-CERT-ICD WP02 database, comments to the manuscript, approval of the final manuscript; member of the EU-CERT-ICD Study team. GS—physiological interpretation of the concepts of ECG analyses, physiological interpretation of the measurement results, completeness control of the data analyses, interpretation of results, manuscript draft, manuscript revisions, approval of the final manuscript; member of the EU-CERT-ICD Study team. CS—responsibility for the work package 02 (retrospective data) of EU-CERT-ICD, collection of ECG signals contributed by the Basel team to the ECG part of the WP02 database of EU-CERT-ICD, submission of these ECGs for study analyses, quality control of the Basel part of the EU-CERT-ICD WP02 ECGs after their conversion into a common open format, follow-up of the Basel patients submitted to the retrospective WP02 part of EU-CERT-ICD, quality control of the complete EU-CERT-ICD WP02 database, comments to the manuscript, approval of the final manuscript; member of the EU-CERT-ICD Study team. MZ—overall responsibility for the EU-CERT-ICD Study, collection of ECG signals contributed by the Göttingen team to the ECG part of the WP02 database of EU-CERT-ICD, submission of these ECGs for the study analyses, quality control of the Göttingen part of the EU-CERT-ICD WP02 ECGs after their conversion into a common open format, follow-up of the Göttingen patients submitted to the retrospective part of EU-CERT-ICD, quality control of the Göttingen part of the EU-CERT-ICD WP02 database, comments to the manuscript, approval of the final manuscript; chair of the

EU-CERT-ICD Study team. MM—proposal of the concept of the ECG analysis, sequential structure of ECG analyses, conceptual design of the study, ECG processing algorithms, software coding and computer implementation of ECG analyses, quality control of the algorithmic measurements of relevant ECG intervals, quality control of the manual adjustments of the measurements of relevant ECG intervals, application of the analytical methods to the EU-CERT-ICD W02 database of ECG signals, interpretation of results, manuscript draft, interpretation and team reporting of review comments, manuscript revisions, approval of individual manuscript versions, study and article guarantor; member of the EU-CERT-ICD Study team.

Funding The EU-CERT-ICD Study was funded by the European Community's 7th Framework Programme (HEALTH-F2-2009-602299). The ECG analyses were supported in part by the British Heart Foundation (NH/16/2/32499), by the Ministry of Health, Czech Republic, conceptual development of research organisation (FNBr/65269705) and by the Specific Research of Masaryk University (MUNI/A/1412/2022).

Competing interests None declared.

Patient and public involvement Patients and/or the public were not involved in the design, or conduct, or reporting, or dissemination plans of this research.

Patient consent for publication Not required.

Ethics approval This study involves human participants and separate ethics approval permissions were obtained by each of the centres contributing the ECG recordings and follow-up data to this study (committees and reference numbers: Basel Ethikkommission Nordwest-und Zentralschweiz (PB_2017-00138); Göttingen Ethikkommission der medizinischen Fakulät Universitätsmedizin Göttingen (22/7/13); Leuven EC University Hospitals Leuven (S55991); Oulu Northern Ostrobothnian hospital district (N/A); Utrecht Medisch Ethische Toetsingscommissie, Utrecht (WAG/mb/20/011346)). All patients included in the retrospective data collection provided written informed consent to have their data researched.

Provenance and peer review Not commissioned; externally peer reviewed.

Data availability statement Data are available upon reasonable request. Data are available upon reasonable request pending the approval by the EU-CERT-ICD Steering Committee.

ORCID iDs
Irena Andršová http://orcid.org/0000-0001-8973-5967
Marek Malik http://orcid.org/0000-0002-3792-1407

REFERENCES

1 Hnatkova K, Andršová I, Toman O, *et al*. Spatial distribution of physiologic 12-lead QRS complex. *Sci Rep* 2021;11:4289.
2 Hnatkova K, Andršová I, Novotný T, *et al*. QRS micro-fragmentation as a mortality Predictor. *Eur Heart J* 2022;43:4177–91.
3 Ray D, Hazra S, Goswami DP, *et al*. An evaluation of Planarity of the spatial QRS loop by three dimensional Vectorcardiography: its emergence and loss. *J Electrocardiol* 2017;50:652–60.
4 Acar B, Yi G, Hnatkova K, *et al*. Spatial, temporal and Wavefront direction characteristics of 12-lead T-wave morphology. *Med Biol Eng Comput* 1999;37:574–84.
5 Sticherling C, Arendacka B, Svendsen JH, *et al*. Sex differences in outcomes of primary prevention Implantable Cardioverter-Defibrillator therapy: combined Registry data from eleven European countries. *Europace* 2018;20:963–70.
6 Johannesen L, Vicente J, Hosseini M, *et al*. Automated algorithm for J-Tpeak and Tpeak-tend assessment of drug-induced Proarrhythmia risk. *PLoS One* 2016;11:e0166925.
7 Dhingra R, Ho Nam B, Benjamin EJ, *et al*. Cross-sectional relations of electrocardiographic QRS duration to left ventricular dimensions: the Framingham heart study. *J Am Coll Cardiol* 2005;45:685–9.
8 Khatib R, Sabir FRN, Omari C, *et al*. Managing drug-induced QT prolongation in clinical practice. *Postgrad Med J* 2021;97:452–8.
9 Tse G, Gong M, Wong WT, *et al*. The T_{Peak} - T_{End} interval as an electrocardiographic risk marker of arrhythmic and mortality outcomes: A systematic review and meta-analysis. *Heart Rhythm* 2017;14:1131–7.
10 Gleeson S, Liao Y-W, Dugo C, *et al*. ECG-derived spatial QRS-T angle is associated with ICD implantation, mortality and heart failure admissions in patients with LV systolic dysfunction. *PLoS One* 2017;12:e0171069.
11 Terho HK, Tikkanen JT, Junttila JM, *et al*. Prevalence and Prognostic significance of fragmented QRS complex in middle-aged subjects with and without clinical or electrocardiographic evidence of cardiac disease. *Am J Cardiol* 2014;114:141–7.
12 Kinugasa Y, Nakamura K, Kamitani H, *et al*. Left ventricular mass index-to-QRS-voltage ratio predicts outcomes in heart failure with preserved ejection fraction. *ESC Heart Fail* 2022;9:1098–106.
13 Marinko S, Platonov PG, Carlson J, *et al*. Baseline QRS area and reduction in QRS area are associated with lower mortality and risk of heart failure hospitalization after cardiac Resynchronization therapy. *Cardiology* 2022;147:298–306.
14 Burgess MJ. Relation of ventricular Repolarization to electrocardiographic T wave-form and arrhythmia vulnerability. *Am J Physiol* 1979;236:H391–402.
15 Rizas KD, McNitt S, Hamm W, *et al*. Prediction of sudden and non-sudden cardiac death in post-infarction patients with reduced left ventricular ejection fraction by periodic Repolarization Dynamics: MADIT-II Substudy. *Eur Heart J* 2017;38:2110–8.
16 Bauer A, Klemm M, Rizas KD, *et al*. Prediction of mortality benefit based on periodic Repolarisation Dynamics in patients undergoing prophylactic implantation of a Defibrillator: a prospective, controlled, Multicentre cohort study. *Lancet* 2019;394:1344–51.
17 Jacquemet V. A simple Analytical model of action potential duration profile in Electrotonically-coupled cells. *Math Biosci* 2016;272:92–9.
18 Yamauchi K. Computer analysis of Vectorcardiograms in myocardial infarction with special reference to polar vector and Planarity of the QRS and T loops. *Jpn Heart J* 1979;20:587–601.
19 Choudhuri S, Ghosal T, Goswami DP, *et al*. Planarity of the spatial QRS loop of Vectorcardiogram is a crucial diagnostic and Prognostic parameter in acute myocardial infarction. *Med Hypotheses* 2019;130:109251.
20 Al-Zaiti SS, Runco KN, Carey MG. Increased T wave complexity can indicate Subclinical myocardial ischemia in asymptomatic adults. *J Electrocardiol* 2011;44:684–8.
21 Zabel M, Acar B, Klingenheben T, *et al*. Analysis of 12-lead T-wave morphology for risk stratification after myocardial infarction. *Circulation* 2000;102:1252–7.
22 Perkiömäki JS, Hyytinen-Oinas M, Karsikas M, *et al*. Usefulness of T-wave loop and QRS complex loop to predict mortality after acute myocardial infarction. *Am J Cardiol* 2006;97:353–60.
23 Okin PM, Malik M, Hnatkova K, *et al*. Repolarization abnormality for prediction of all-cause and cardiovascular mortality in American Indians: the strong heart study. *J Cardiovasc Electrophysiol* 2005;16:945–51.
24 Seegers J, Hnatkova K, Friede T, *et al*. T-wave loop area from a pre-implant 12-lead ECG is associated with appropriate ICD shocks. *PLoS One* 2017;12:e0173868.
25 Pelli A, Kenttä TV, Junttila MJ, *et al*. Electrocardiogram as a Predictor of survival without appropriate shocks in primary prophylactic ICD patients: A retrospective multi-center study. *Int J Cardiol* 2020;309:78–83.
26 Bauer A, Barthel P, Müller A, *et al*. Risk prediction by heart rate turbulence and deceleration capacity in postinfarction patients with preserved left ventricular function retrospective analysis of 4 independent trials. *J Electrocardiol* 2009;42:597–601.
27 Malik M, Kulakowski P, Poloniecki J, *et al*. Frequency versus time domain analysis of signal-averaged electrocardiograms. *J Am Coll Cardiol* 1992;20:127–34.
28 Younis A, Goldberger JJ, Kutyifa V, *et al*. Predicted benefit of an Implantable Cardioverter-Defibrillator: the MADIT-ICD benefit score. *Eur Heart J* 2021;42:1676–84.
29 Zabel M, Willems R, Lubinski A, *et al*. Clinical effectiveness of primary prevention Implantable Cardioverter-Defibrillators: results of the EU-CERT-ICD controlled Multicentre cohort study. *Eur Heart J* 2020;41:3437–47.

QRS complex and T wave planarity for the efficacy prediction of automatic implantable defibrillators

by

Katerina Hnatkova[A], Irena Andršová[B,C], Tomáš Novotný[B,C], Bert Vandenberk[D], David J Sprenkeler[E], Juhani Junttila[F], Tobias Reichlin[G], Simon Schlögl[H,I], Marc A Vos[E], Tim Friede[J,I], Axel Bauer[K], Heikki V Huikuri[F], Rik Willems[D], Georg Schmidt[L,M], Christian Sticherling[N], Markus Zabel[H,I], Marek Malik[A,B,C], on behalf of EU-CERT-ICD investigators

[A] National Heart and Lung Institute, Imperial College, London, England,
[B] Department of Internal Medicine and Cardiology, University Hospital Brno, Brno, Czech Republic,
[C] Department of Internal Medicine and Cardiology, Masaryk University, Brno, Czech Republic,
[D] Department of Cardiovascular Sciences, University of Leuven, Leuven, Belgium,
[E] Department of Medical Physiology, University Medical Center Utrecht, Utrecht, The Netherlands,
[F] University Central Hospital of Oulu and University of Oulu, Finland,
[G] Department of Cardiology, Inselspital, Bern University Hospital, Bern, Switzerland
[H] Department of Cardiology and Pneumology, University Medical Center, Göttingen, Germany,
[I] German Center of Cardiovascular Research (DZHK), partner site Göttingen, Göttingen, Germany
[J] Department of Medical Statistics, University Medical Center Göttingen, Göttingen, Germany
[K] University Hospital for Internal Medicine III, Medical University Innsbruck, Innsbruck, Austria,
[L] Klinikum rechts der Isar, Technical University of Munich, Munich, Germany,
[M] German Center for Cardiovascular Research partner site Munich Heart Alliance, Munich, Germany,
[N] Department of Cardiology, University Hospital of Basel, Basel, Switzerland.

Supplementary material

ECG loop planarity measurement

The standard 12-lead ECG contains only 8 algebraically independent leads I, II, V1, V2, …, V6 since the unipolar limb leads are only simple algebraic combinations of leads I and II. Hence, the ECG signal may be considered to constitute a matrix $\mathbb{M}^{8,n}$ of voltage values which has 8 rows $\mathbb{m}_i$ corresponding to individual leads, and n columns, each corresponding to one time-instant. That is, each row $\mathbb{m}_i$ is a function of time and the values $\mathbb{m}_i(t)$, where $0 \leq t < n$, create the image of the i-th lead of the original ECG recording. The singular value decomposition is based on an algorithm that creates a diagonal matrix $\mathbf{\Sigma}^{8,n}$ and matrices $\mathbb{U}^{8,8}$ and $\mathbb{V}^{n,n}$ such that $\mathbf{\Sigma} = \mathbb{U}^T\mathbb{M}\mathbb{V}$, which means $\mathbb{M} = \mathbb{U}\mathbb{W}$, where $\mathbb{W}^{8,n} = \mathbf{\Sigma}\mathbb{V}^T$. Σ is a diagonal matrix with non-zero values only in the left-most diagonal. These elements of $\mathbf{\Sigma}$ (all > 0) are the eigenvalues $\{\sigma_i\}_{i=1}^{8}$ of the decomposition while the columns of matrices $\mathbb{U}$ and $\mathbb{V}$ are the left and right singular vectors. The rows of matrix $\mathbb{W}$ are the algebraically orthogonal components $\{\lambda_i\}_{i=1}^{8}$ of the decomposition.

In the signal analyses described in this study, the singular value decomposition was applied to the representative beatforms of each ECG, as described in the main article text.

Original beatform signal in matrix $\mathbb{M}$ can be reconstructed using only a subset of the components of orthogonal signal matrix $\mathbb{W}$. Specifically, for any subset of the 8 orthogonal components (i.e., any selection of one, two, or more of the components λ_i), a matrix $\mathbb{X}^{8,n}$ can be created, for which the rows of the subset are the same as the corresponding rows of $\mathbb{W}$ while other rows contain zeros. The original matrix $\mathbb{M}$ can then be approximated by matrix $\mathbb{N}^{8,n} = \mathbb{U}\mathbb{X}$. Each of the 8 rows of matrix $\mathbb{N}$ correspond to the approximation of the corresponding ECG lead that originally constituted the matrix $\mathbb{M}$.

To quantify the difference between $\mathbb{M}$ and $\mathbb{N}$ signals, this study calculated the area between the signals of individual leads of $\mathbb{M}$ and $\mathbb{N}$. That is for each lead $l \in \{\mathrm{I}, \mathrm{II}, \mathrm{V1}, \mathrm{V2}, \ldots, \mathrm{V6}\}$, the difference Δ_l was calculated between original lead $\mathbb{m}_l$ and its approximation $\mathbb{n}_l$ as $\Delta_l = \sum_{t=0}^{n-1}|\mathbb{m}_l(t) - \mathbb{n}_l(t)|$ and the overall difference $\mathbf{\Delta}$ between $\mathbb{M}$ and $\mathbb{N}$ was calculated as the average of all Δ_l (i.e., the average over different algebraically independent leads).

If the selected subset of the 8 orthogonal components was empty, the matrix $\mathbb{N}$ contained only zeros and all $\Delta_l = \sum_{t=0}^{n-1}|\mathbb{m}_l(t)|$.

This allowed to order the orthogonal components $\{\lambda_i\}_{i=1}^{8}$ according to their contribution to the original ECG signal. That is, we firstly selected a single component λ_{1st} such that if only this component was used in matrix $\mathbb{X}$, the corresponding $\mathbb{N}$ to $\mathbb{M}$ difference $\mathbf{\Delta}$ was the smallest among all single components λ_i. Subsequently, we selected a second component λ_{2nd} such that if the matrix $\mathbb{X}$

was composed of components ($\lambda_{1st} \oplus \lambda_{2nd}$) – i.e. if the matrix $\mathbb{X}$ had only two non-zero rows, the corresponding $\mathbb{N}$ to $\mathbb{M}$ difference $\boldsymbol{\Delta}$ was the smallest among all two component combinations ($\lambda_{1st} \oplus \lambda_i$), where $\lambda_i \neq \lambda_{1st}$. The same process was repeated and λ_{3rd} was selected for minimum approximation difference based on ($\lambda_{1st} \oplus \lambda_{2nd} \oplus \lambda_{3rd}$), and so on, up to the selection of the last λ_{8th} orthogonal component. This results in an order of decomposing components $\{\lambda^{(j)}\}_{j=1}^{8}$, where $\lambda^{(1)} = \lambda_{1st}$, $\lambda^{(2)} = \lambda_{2nd}$, and so on.

This selection of λ components results in a sequence of $\mathbb{N}$ to $\mathbb{M}$ differences $\{\boldsymbol{\Delta}_i\}_{i=0}^{8}$ where $\boldsymbol{\Delta}_i$ corresponds to the approximation signals $\mathbb{N}$ composed of the first i components selected during the described selection process. Clearly $\boldsymbol{\Delta}_0 \geq \boldsymbol{\Delta}_1 \geq \boldsymbol{\Delta}_2 \geq \cdots \geq \boldsymbol{\Delta}_8 = 0$. The absolute contribution of the i-th component to the reconstruction of original ECG signal $\mathbb{M}$ is equal to $\boldsymbol{\Delta}_{i-1} - \boldsymbol{\Delta}_i$. Clearly, the value of this absolute contribution depends on the magnitude of the original ECG and cannot be directly used for comparisons of different ECGs. For that purpose, it is appropriate to consider the contribution of the i-th component in relative terms, i.e., as a value $\boldsymbol{\nabla}_i = (\boldsymbol{\Delta}_{i-1} - \boldsymbol{\Delta}_i)/\boldsymbol{\Delta}_0$.

This order of the decomposing components allows to construct a 3-dimensional ECG loop using components $\lambda^{(1)}$, $\lambda^{(2)}$, and $\lambda^{(3)}$. Of these, the components $\lambda^{(1)}$ and $\lambda^{(2)}$ defined the 2-dimensional plane of the vector movement while component $\lambda^{(3)}$ corresponded to the twist of the 3-dimensional loop out of the $\lambda^{(1)}$ + $\lambda^{(2)}$ plane. Correspondingly, the non-planarity of the vector loop was numerically quantified by the value $\boldsymbol{\nabla}_3$.

When only three independent leads were used modelling the signals between the chest belt electrodes, exactly the same principles were used. The only difference was that the source matrix $\mathbb{M}^{3,n}$ with only 3 rows was considered and thus, only three decomposing components $\{\lambda^{(j)}\}_{j=1}^{3}$ were obtained.

Regardless of whether 8 or only 3 independent ECG leads were used, the values $\boldsymbol{\nabla}_3$ were obtained using matrices that spanned between the QRS onset and QRS offset, and between the QRS offset and T wave offset.

The examples of 3-dimensional loops shown in Figure 1 of the main article were derived by this signal value decomposition analysis applied to source ECGs shown in Supplementary Figure 1. (Although the source ECGs were of 10-second duration, only 5-second signals are shown in Supplementary Figure 1). The representative beatforms that were processed by the signal value decomposition to create the loops shown in Figure 1 of the main article are presented in Supplementary Figure 2. Note that the differentiation between the QRS loop twists is impossible to judge visually in the Supplementary Figures 1 and 2. See also the supplementary animations.

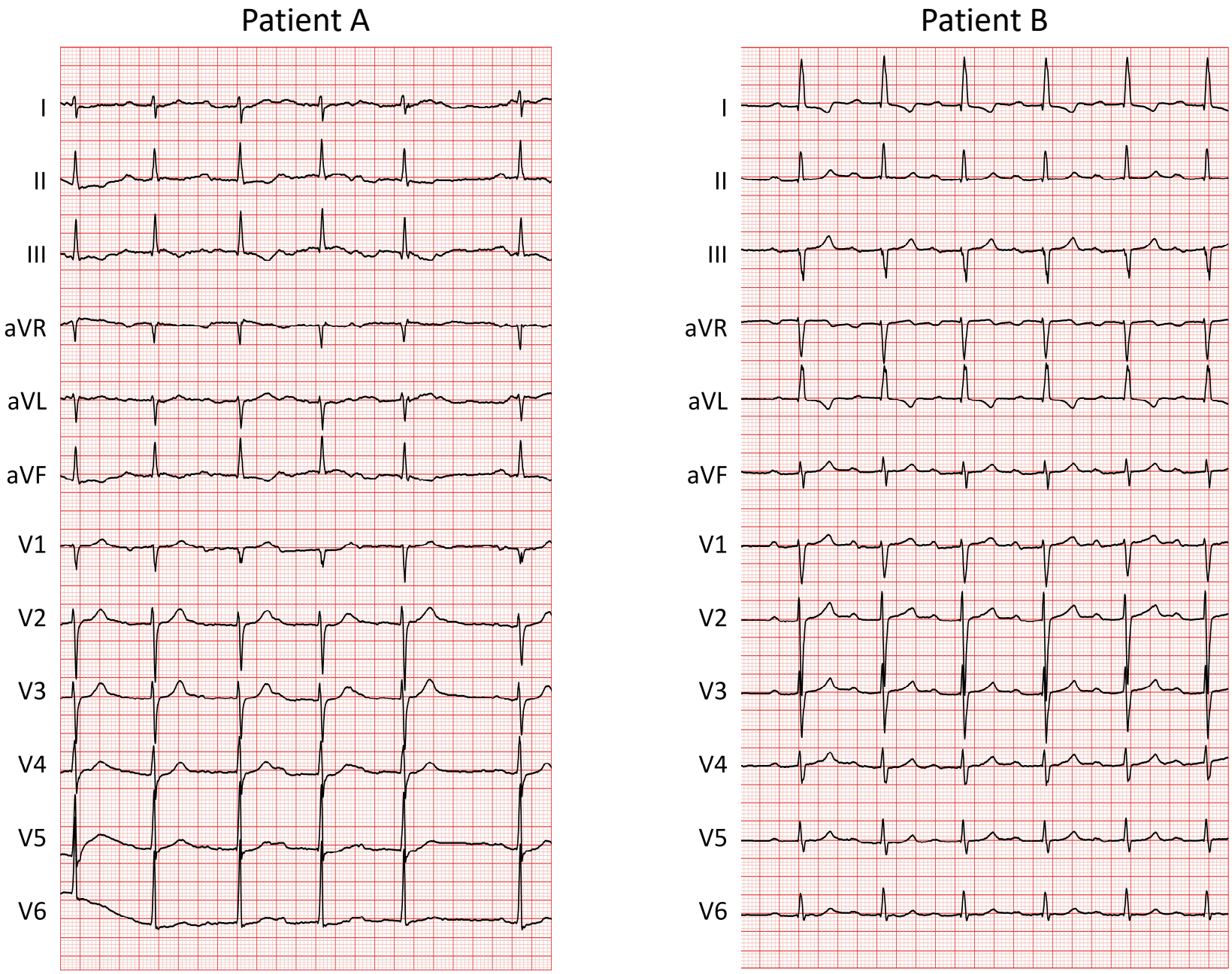

Supplementary Figure 1

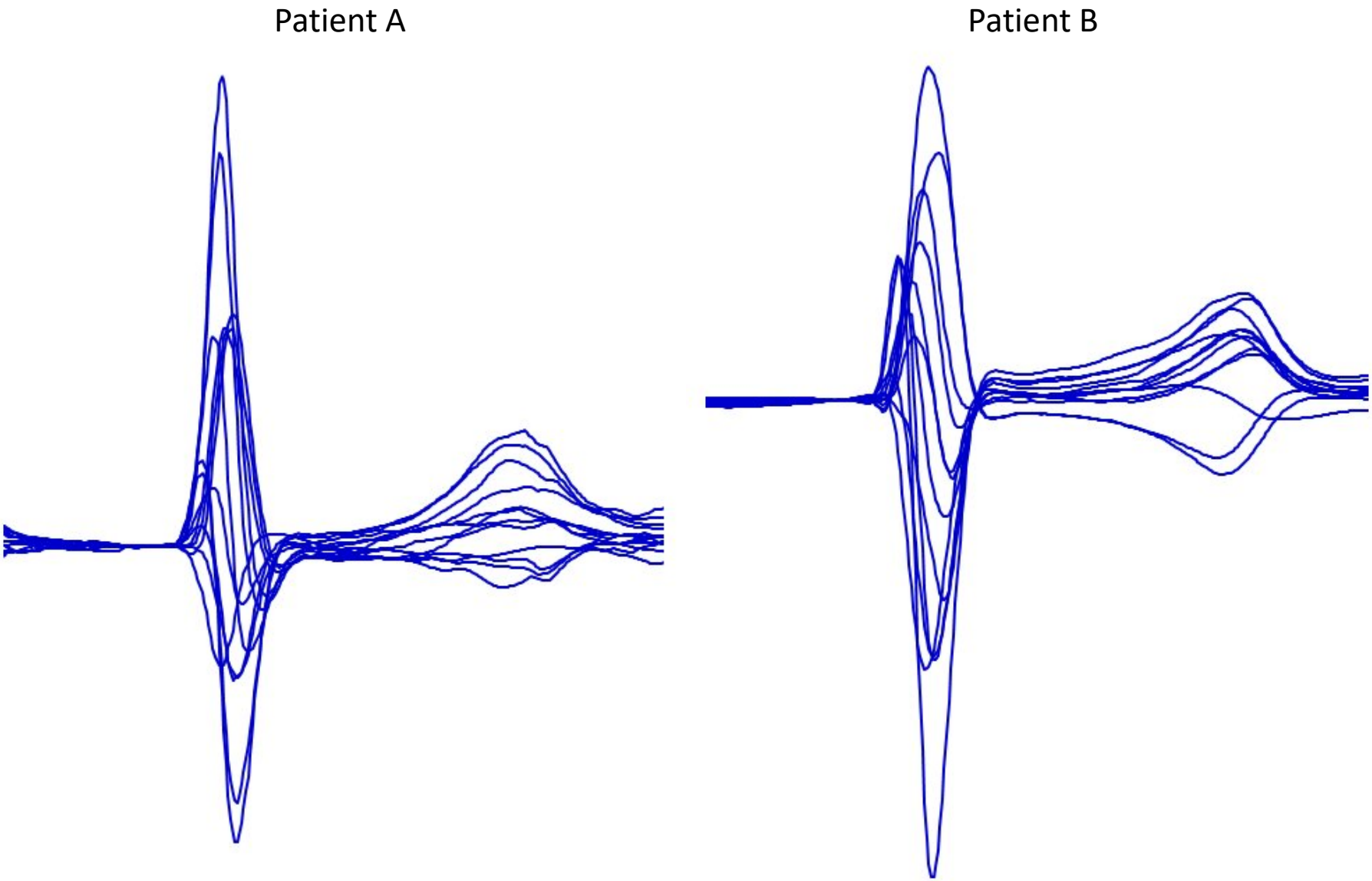

Supplementary Figure 2

Additional data analyses

The comparisons of QRS complex non-planarity values and T wave non-planarity values in patients who did and did not survive during the study follow-up and in patients who experienced and did not experience appropriate ICD shocks, as shown for the values derived from original 12-lead ECGs in Figure 2 of the main article, were repeated for the values derived from the three independent leads modelling the signals between the chest belt electrodes.

As explained in the main article, there were 45 patients who received an appropriate ICD shock but subsequently died before the end of the follow-up. The Kaplan-Meier analyses of the probability of death despite ICD protection, and of the probability of first appropriate ICD shock, as presented in Figures 3 and 4 of the main article, were therefore repeated in populations of patients who did not receive any appropriate ICD shocks during the follow-up (for the comparisons of the probability of death) and who did not die during the follow-up (for the comparisons of the probability of receiving an appropriate ICD shock).

Receiver operator characteristics (i.e., dependencies of specificity on sensitivity) were calculated for the prediction of all-cause mortality and of appropriate ICD shocks before the end of follow-up. These characteristics of the prediction of death were calculated using QRS complex non-planarity data and for the combinations of QRS complex non-planarity with heart rate and the QRS-T angle. The characteristic of the prediction of appropriate ICD shocks was calculated using T wave non-planarity data. The selection of the characteristics used in these calculations was derived from the Cox regression results presented in Table 2 of the main manuscript (while using only ECG-derived data). The characteristics were calculated using the non-planarity measurement derived from the complete 12-lead ECG signals (i.e., from the 8 algebraically independent leads).

The calculation of receiver operator characteristics was performed together with their dual-sided empirical 95% confidence bands. These were calculated using a bootstrap technique with 1000 repetitions. For the calculation of multivariable receiver operator characteristics based on n numerical indices, definition of positive test distinguished between number of m positive comparisons. That is, for the different indices $\{\mathcal{J}_i\}_{i=1}^{n}$, their dichotomies $\{\mathfrak{d}_i\}_{i=1}^{n}$ were varied and for each setting of the dichotomies, the multivariable test was considered positive if $\mathcal{J}_i \geq \mathfrak{d}_i$ for at least m indices. The required number m of positive results was varied between 1 and n.

Applying these general principles to the data of the present study meant that for the combination of heart rate, QRS-T angle, and QRS loop non-planarity, the dichotomies were varied, and the multivariable test was considered positive if 1, or 2, or 3 of these indices were above the

corresponding dichotomy. Since the study date included 294 patients who died during the follow-up, 294 different dichotomies of each of the index had to be considered, leading to 294^3 = 25,412,184 combinations that had to be evaluated to obtain the full sensitivity / specificity profile.

Harrel's concordance index C was computed to further assess discrimination of the risk predictors. This was calculated for QRS-loop non-planarity and T-wave-loop non-planarity used as predictors of all-cause mortality and appropriate ICD shocks. Bootstrap technique with 1000 repetitions was used to obtain confidence intervals of the C index values.

To calibrate the risk predictors, the study population was sorted according to either the QRS-loop non-planarity values or to the T-wave-loop non-planarity values. For both these possibilities, quintiles of the population were considered (numbered 1^{st} with the lowest and 5^{th} with the highest non-planarity values, respectively) and in each quintile, the observed incidence of all-cause mortality and of first appropriate ICD shocks was counted. The non-uniformity of the distribution of these incidence counts was tested using chi-square test.

As explained in the main document, defibrillators with 797 patients (40.9%) were implanted defibrillators with cardiac resynchronisation therapy (CRT) function. The follow-up incidence of all-cause mortality and of appropriate ICD shocks was compared between patients with and without CRT defibrillators. The comparison was based on Kaplan-Meier curves of even probabilities. The comparisons of death probabilities between patients with QRS loop non-planarity above and below population median was also performed separately among patients with and without CRT defibrillators.

Additional results

Supplementary Figure 3 shows the comparisons of QRS complex non-planarity values (panels A and B) and T wave non-planarity values (panels C and D) in patients who did and did not survive during the study follow-up (panels A and C) and in patients who experienced and did not experience appropriate ICD shocks (panels B and D). In each panel, cumulative distributions of the non-planarity values are shown together with Kolmogorov-Smirnov statistics and their corresponding p-values. The non-planarity values shown were derived from the analysis of all 3 independent leads modelling chest belt recordings.

Supplementary Figure 4 shows Kaplan-Meier analyses of the probability of death despite ICD protection (panels A and C) among patients who did not experience any appropriate ICD shocks during study follow-up. The figure further shows Kaplan-Meier analysis of the probability of first appropriate ICD shock (panels B and D) among patients who survived during the study follow-up.

Panels A and B compare the sub-groups stratified by QRS complex non-planarity (QRS loop twist), panels C and D compare the sub-groups stratified by the T wave non-planarity (T wave loop twist). The characteristics used in the comparisons were derived from 8 independent leads of the complete ECG recordings. Chi-square statistics and corresponding p-values comparing the Kaplan-Meier curves are shown in each panel. The number of patients at risk in these groups are shown below the panels in colours corresponding to the individual graphs. Supplementary Figure 5 shows the same Kaplan-Meier analyses as presented in Supplementary Figure 4 but instead of characteristics derived from 8 independent leads of the complete ECG recordings, it shows the comparisons based on characteristics derived from the analysis of all 3 independent leads modelling the chest belt recordings.

Supplementary Figure 6 shows the receiver operator characteristics for the prediction of all-cause mortality during study follow-up (panels A, B, and C) and for the prediction of appropriate ICD shocks (panel D). In all panels, the characteristic is shown together with its empirical 95% dual-sided confidence band. Area under the characteristic curve (and the corresponding 95% confidence interval) are shown in each panel. Panel A shows the characteristic derived from QRS loop non-planarity values while panels B and C show multivariable characteristics derived from a combination of the QRS loop non-planarity with heart rate and QRS-T angle values (options 2 out of 3 positive and 3 out of 3 positive are shown in panels B and C, respectively). These panels show that in terms of the receiver operator characteristics, the QRS loop non-planarity adds meaningfully to other ECG-based risk factors. The characteristic for the prediction of appropriate ICD shocks shown in Panel D was derived from the T wave loop non-planarity. The T wave loop non-planarity was the only ECG-based factor that led to a receiver operator characteristic with the area under the characteristic being significantly larger than 0.5.

The Harrel's concordance index C values (and their 95% confidence intervals) for all-cause mortality prediction by QRS-loop non-planarity, all-cause mortality prediction by T-wave-loop non-planarity, first appropriate ICD shock prediction by QRS-loop non-planarity, and first appropriate ICD shock prediction by QRS-loop non-planarity were 0.575 (0.542 - 0.605), 0.526 (0.493 - 0.560), 0.554 (0.512 - 0.595), and 0.568 (0.528 - 0.608), respectively.

Supplementary Figure 7 shows the incidence of all-cause mortality (red bars in panels A and C) and of first appropriate ICD shocks (blue bars in panels B and D) in populations quintiles sorted by QRS-loop non-planarity values (top panels A and B) and by T-wave-loop non-planarity values (bottom panels C and D). Chi-square p-values of the tests of distribution uniformity are shown in each panel. The differences from uniform distribution across the quintiles were all statistically significant apart

from the distribution of all-cause mortality in quintiles according to the T-wave-loop non-planarity values (Panel C).

Supplementary Figure 8 shows the Kaplan-Meier comparisons of follow-up all-cause mortality and of appropriate ICD shocks between patients with CRT and non-CRT defibrillators (panels A and B), and of the mortality differences between patients with QRS loop non-planarity below and above population median separately in patients with non-CRT defibrillators (panel C) and in patients with CRT-defibrillators (panel D). The number of patients at risk in these groups are shown below the panels in colours corresponding to the individual graphs. While the probability of all-cause mortality was significantly increased in patients with CRT defibrillators (panel A), there was only a borderline trend towards fewer appropriate ICD shocks among patients with CRT defibrillators (panel B). Panels C and D show that the mortality risk prediction by QRS loop non-planarity was maintained irrespective of whether the patients received CRT or non-CRT defibrillators. Since the CRT/non-CRT defibrillator type had only a non-significant influence on the probability of first appropriate ICD shocks, it was not surprising that the probability of the appropriate shocks was equally stratified by T wave loop non-planarity in both subgroups of patients who received CRT or non-CRT defibrillators (details not shown).

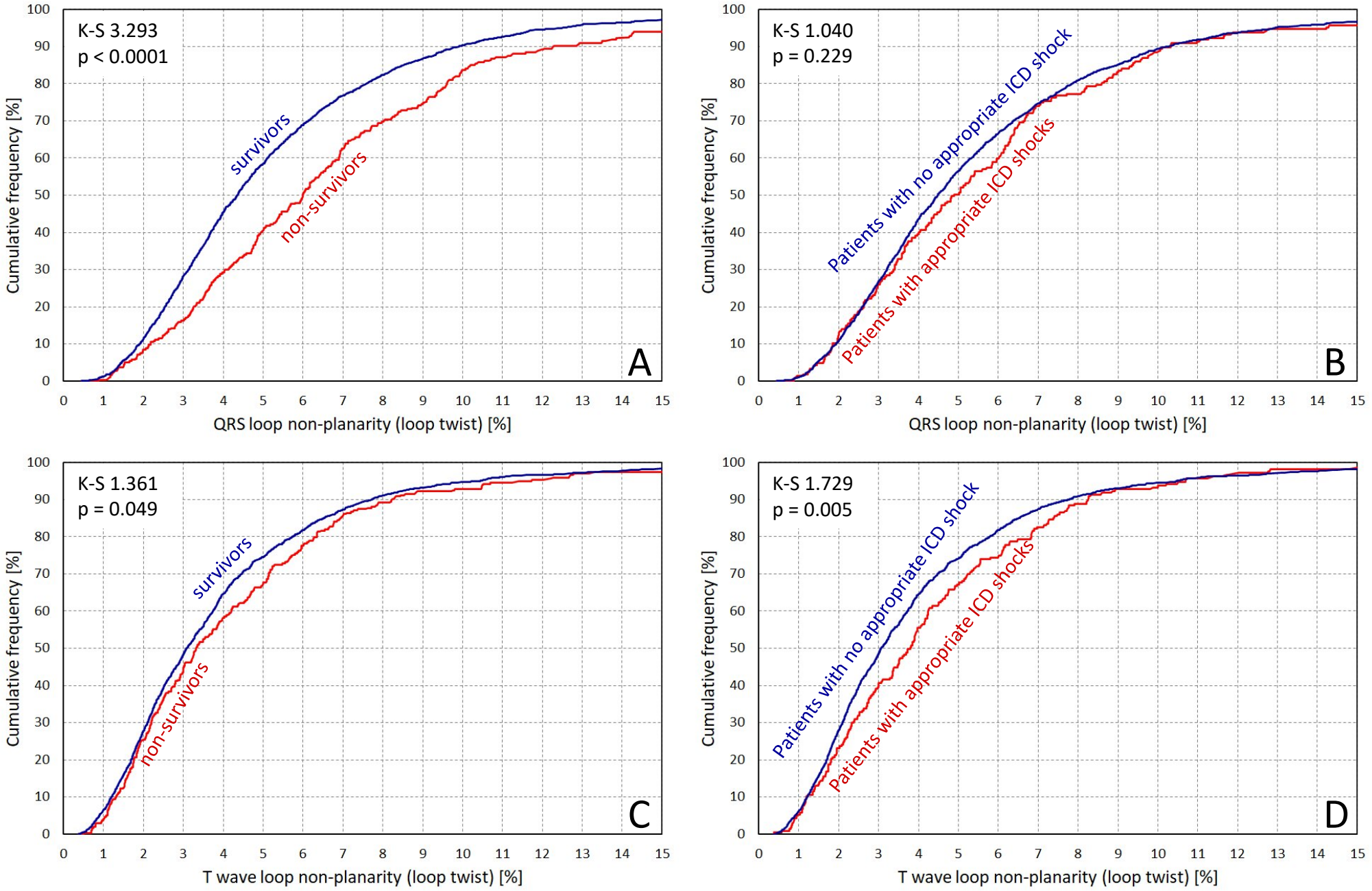

Supplementary Figure 3

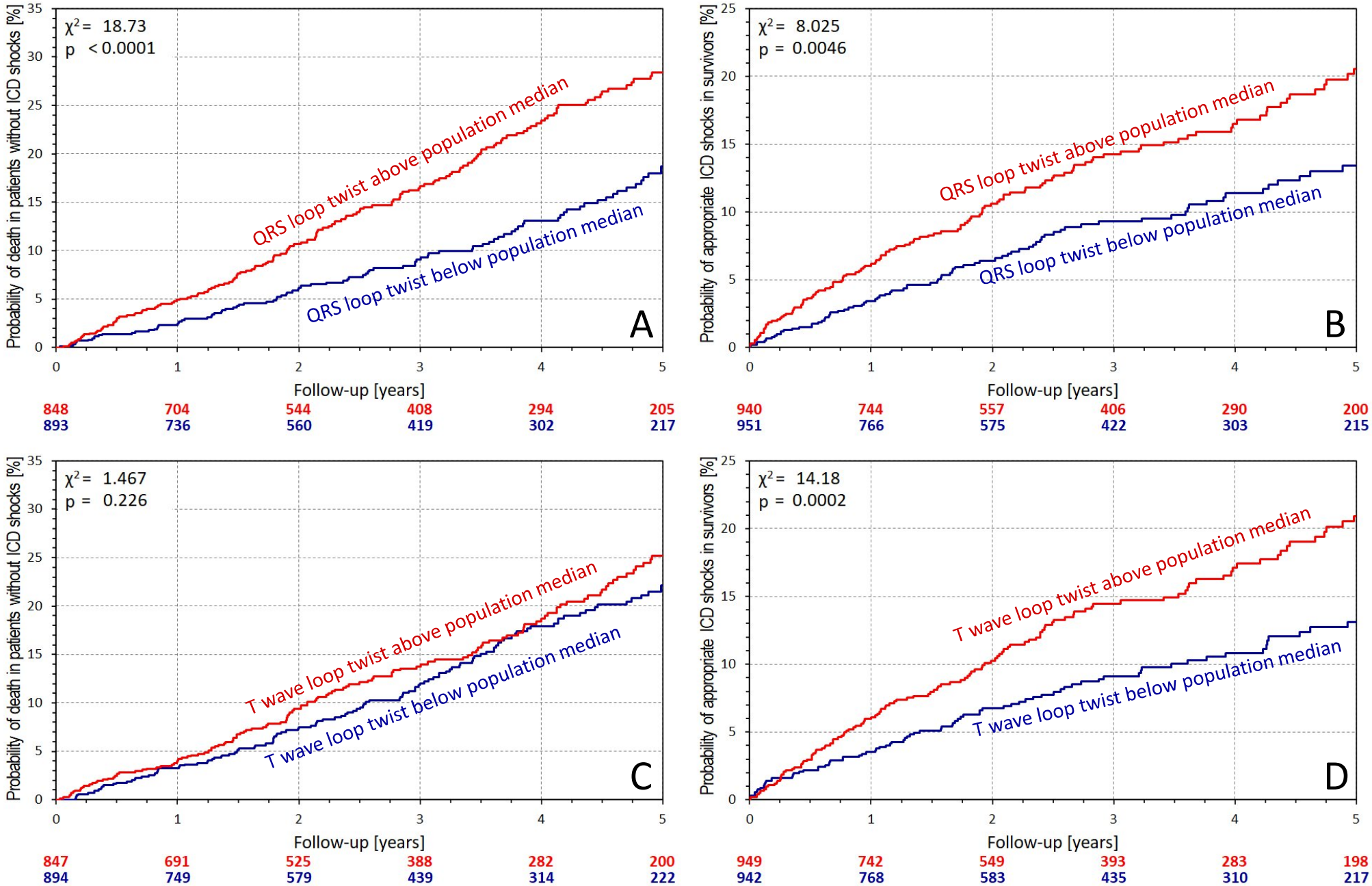

Supplementary Figure 4

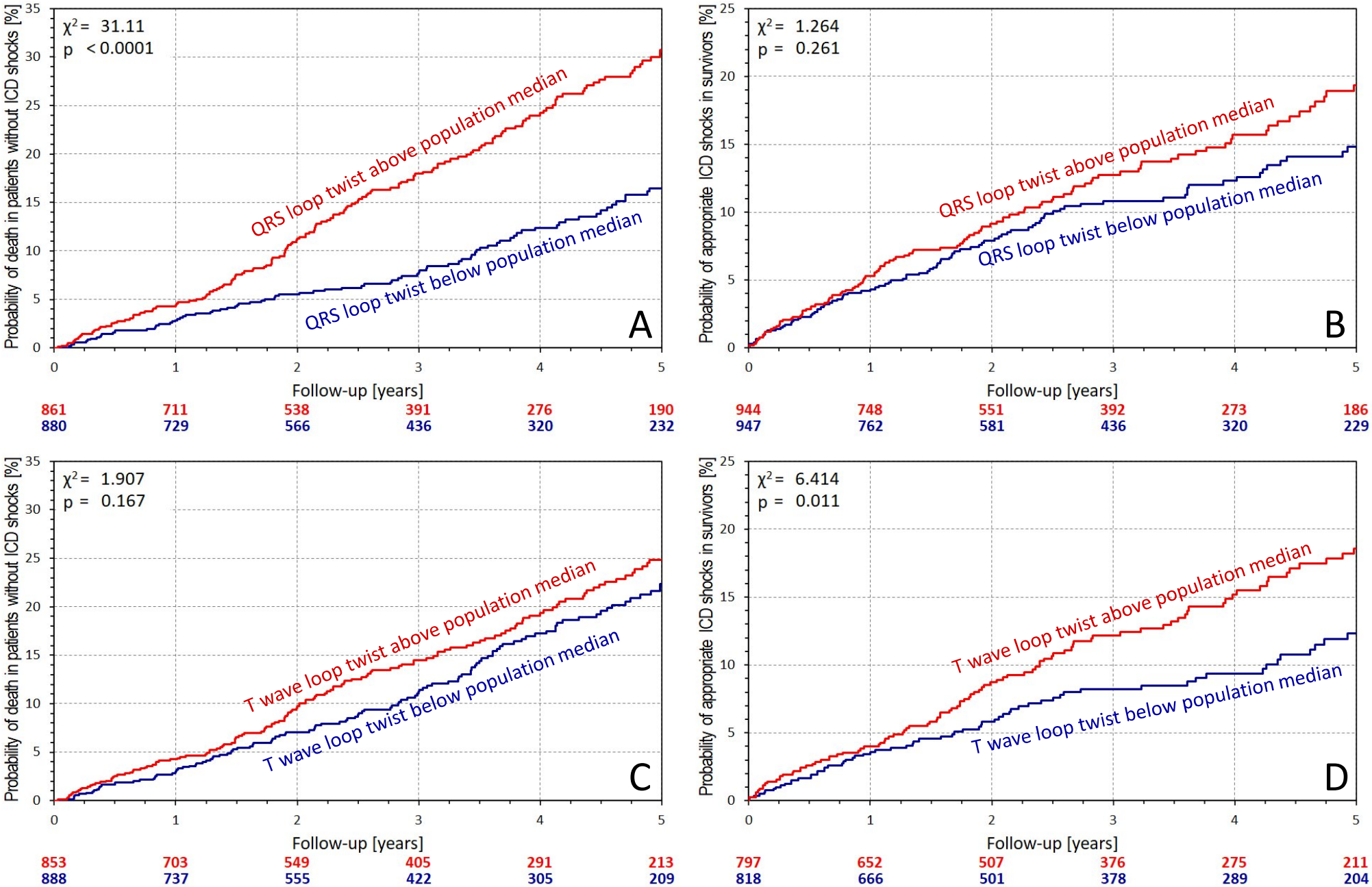

Supplementary Figure 5

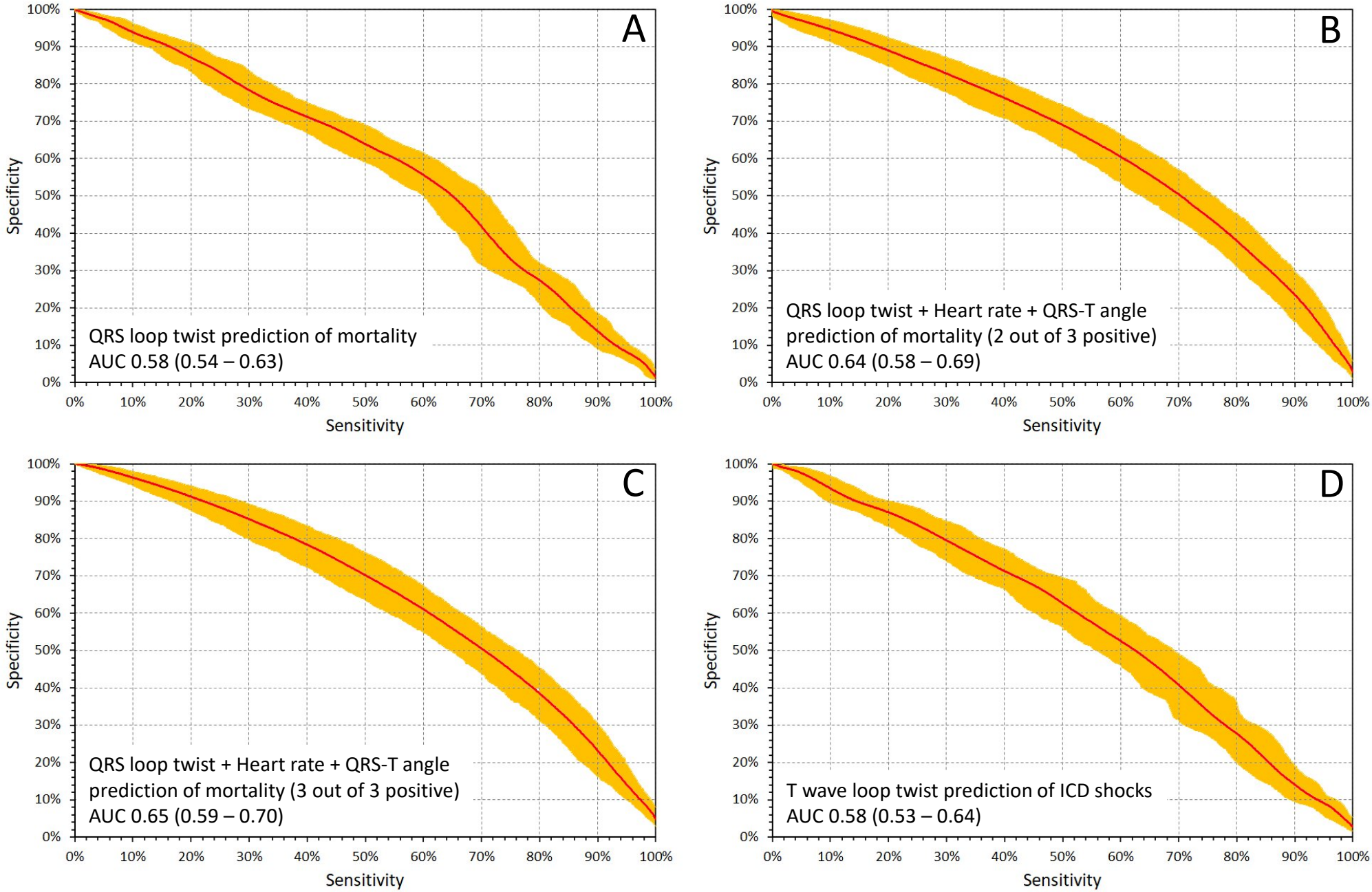

Supplementary Figure 6

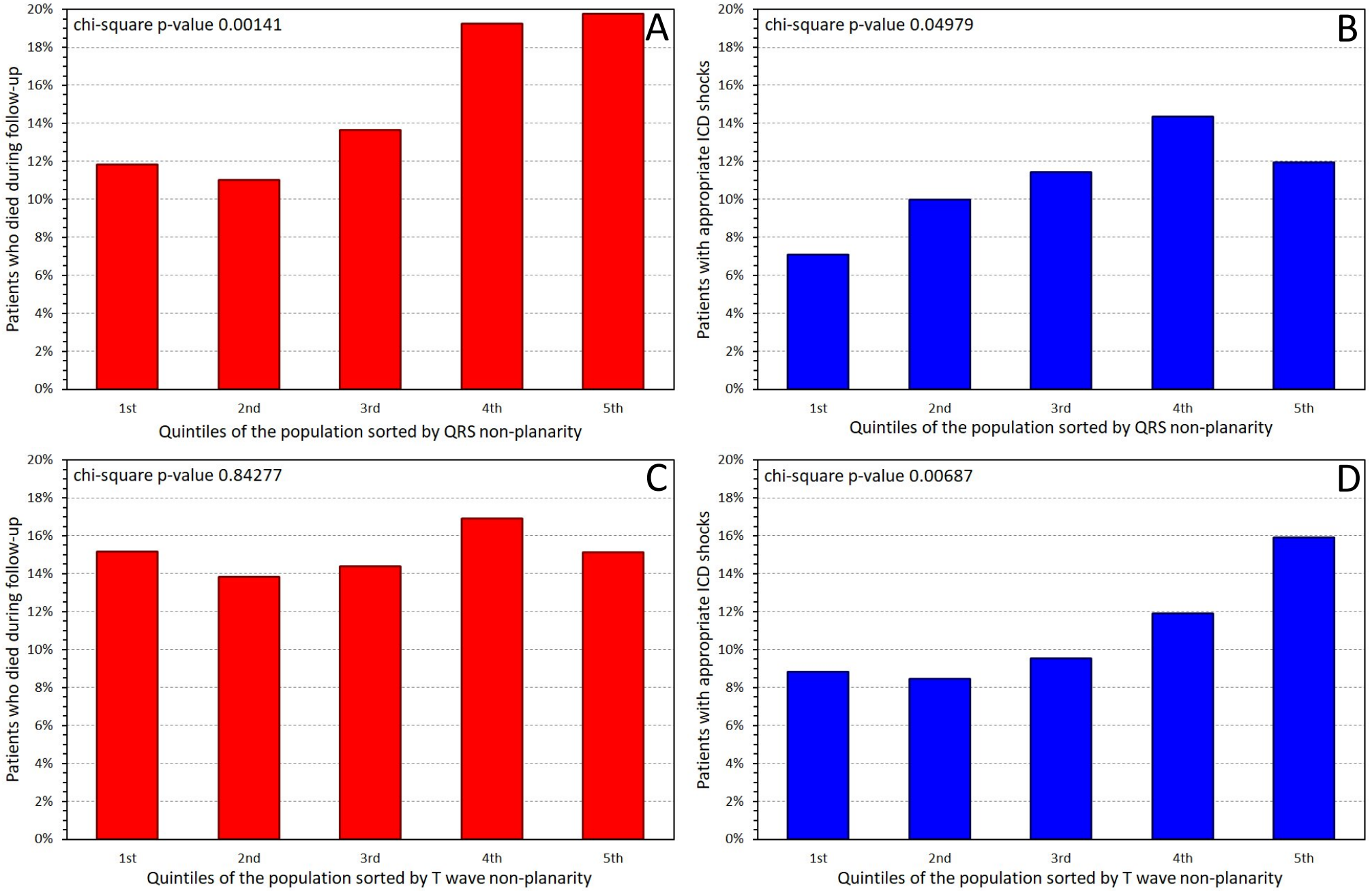

Supplementary Figure 7

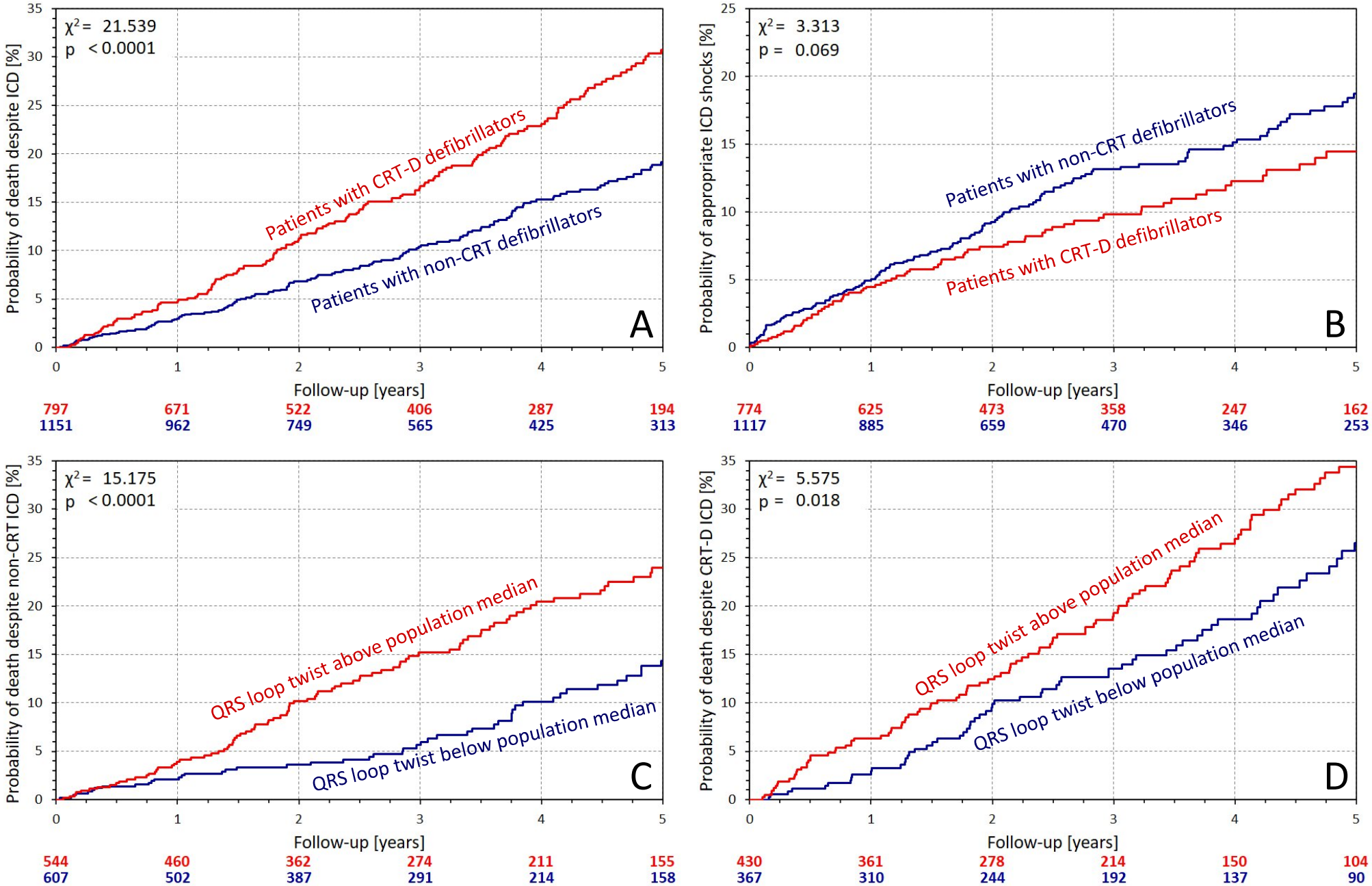

Supplementary Figure 8